Available online at www.sciencedirect.com
ScienceDirect
Precambrian Research 150 (2006) 153–172
Precambrian Research
www.elsevier.com/locate/precamres

# Preservation of Palaeoproterozoic early Svecofennian structures in the Orijärvi area, SW Finland—Evidence for polyphase strain partitioning

Pietari Skyttä [a,*], Markku Väisänen [b], Irmeli Mänttäri [a]

[a] *Geological Survey of Finland, P.O. Box 96, FI-02151 Espoo, Finland*
[b] *Department of Geology, University of Turku, FI-20014 Turku, Finland*

Received 24 February 2006; received in revised form 5 July 2006; accepted 18 July 2006

**Abstract**

The predominantly migmatitic Palaeoproterozoic Uusimaa belt preserves early lower-grade Svecofennian structures in the Orijärvi area in SW Finland. This study aims at explaining the deformational history responsible for its preservation and also at defining the age of the early Svecofennian deformation. Detailed structural analysis reveals that the preservation was enabled by polyphase strain partitioning, which initiated during the early Svecofennian $D_2$ deformation, ~1875 Ma ago, as revealed by ion microprobe U–Pb data on zircons from granodioritic and intermediate syn-$D_2$ intrusive dykes. The $D_2$ structures were low-strain upright folds at high crustal levels and sub-horizontal high-strain folds at deeper crustal levels. The sub-horizontal $D_2$ structures were refolded into upright folds during the subsequent late Svecofennian $D_3$ deformation, whereas the upright $D_2$ structures behaved as almost rigid blocks that caused strain partitioning into high-strain zones along the block margins. This accounts for the low cumulative strain in specific parts of the Orijärvi area. Further strain partitioning during $D_4$ caused reverse dip-slip movements along regional-scale shear zones. Crustal depth controlled the metamorphic grade during $D_2$, when local migmatisation took place at deep crustal levels. Later metamorphic overprint during $D_3$ deformation is evident from post-$D_2$ growth of sillimanite and a second generation of andalusite.

Similarities in the structural patterns between the Orijärvi area and the Tampere-Vammala area (~100 km to the north) suggest that irrespective of the age of the later overprint, subsequent deformation was localised along the margins of the early formed upright domains, while the low-grade rocks within the domains were preserved.
© 2006 Elsevier B.V. All rights reserved.

*Keywords:* Structural geology; Tectonics; Fennoscandian Shield; Ion microprobe; Zircon; U–Pb

## 1. Introduction

The poly-deformed bedrock of southern Finland plays a key role in understanding the Palaeoproterozoic tectonic evolution of the Fennoscandian Shield. Within the present study area, two major events deformed the crust during a period from ~1.89 to 1.81 Ga: The early Svecofennian event at ~1.89–1.86 Ga (Hopgood et al., 1983; Ehlers et al., 2004), and the late Svecofennian tectono-thermal event at ~1840–1815 Ma (Ehlers et al., 1993; Korsman et al., 1999; Levin et al., 2005; Mouri et al., 2005) when high heat flow and associated crustal melting effectively destroyed the older deformation structures. However, the early stages without migmatisation, are well preserved in places such as the Orijärvi area within the Uusimaa belt (Fig. 1;

* Corresponding author. Present address: Department of Civil and Environmental Engineering, Helsinki University of Technology, P.O. Box 6200, FI-02015 TKK, Finland. Tel.: +358 9 4512725; fax: +358 9 4512731.
*E-mail address:* pietari.skytta@tkk.fi (P. Skyttä).

0301-9268/$ – see front matter © 2006 Elsevier B.V. All rights reserved.
doi:10.1016/j.precamres.2006.07.005

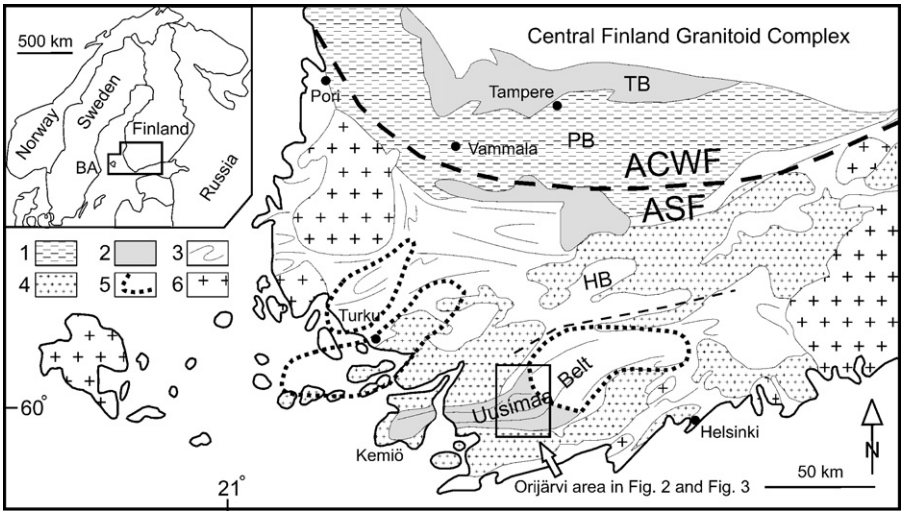


Fig. 1. Generalised geology of southern Finland after Korsman et al. (1997) and Väisänen and Hölttä (1999). Key: (1) tonalitic migmatites, (2) lower amphibolite facies schists, (3) granitic migmatites and other upper amphibolite facies gneisses, (4) late Svecofennian granites ca 1.85–1.81 Ga, (5) granulites, (6) Rapakivi granites (Mesoproterozoic); ACWF = Arc Complex of Central and Western Finland, ASF = Arc Complex of Southern Finland, TB = Tampere belt, PB = Pirkanmaa belt, HB = Häme belt, BA = Bergslagen area (inset). The suture line separating the ACWF and ASF by Lahtinen (1996).

Ploegsma and Westra, 1990; Stel et al., 1999; Väisänen and Mänttäri, 2002; Skyttä et al., 2005), also known as the classical area of metamorphic facies studies by Eskola (1914,1915). Localised preservation of the early Svecofennian structures led to an interest in studying the contrasting tectonic evolution within the well-preserved parts of the Orijärvi area and within the predominantly migmatitic surroundings. Recognition of the different structural domains is particularly important as the two main tectonic events, the early Svecofennian $D_1$–$D_2$ and the late Svecofennian $D_3$–$D_4$, share approximately the same geometrical properties in many places. The mutual geometrical relationships of the domains are used to provide some tectonic constraints on the preservation of the early structures and regional kinematics of the deformations. These will then be applied in correlating the specific well-preserved, low-strain parts of the Orijärvi area in a wider regional context. Two regional-scale shear zones, the Kisko shear zone and the Jyly shear zone (Fig. 2), have a major significance on the structural evolution of the study area as they separate the early, lower grade and the migmatitic domains. In addition, characteristics of the early tectonic events will be further specified. Another main aim of this investigation was to determine the age of the early Svecofennian deformation within the preserved area. The methods of this study include structural and lithological field mapping, structures in thin sections, and ion microprobe dating of two samples by U–Pb system on zircons.

## 2. Geological setting

The Fennoscandian tectonic evolution during the Palaeoproterozoic has earlier been attributed to semi-continuous, protracted Svecofennian orogenesis (Gorbatschev and Bogdanova, 1993). The recent model by Lahtinen et al. (2005), however, includes five separate orogens between 1.92–1.79 Ga; the orogenic evolution was divided into microcontinent accretion stage (1.92–1.87 Ga), continental extension stage (1.86–1.84 Ga), continent-continent collision stage (1.84–1.79 Ga) and orogenic collapse and stabilisation stage (1.79–1.77 Ga). The Uusimaa and Häme belts of the Arc Complex of Southern Finland experienced early Svecofennian event at ~1.89–1.87 Ga (Fennian orogeny by Lahtinen et al. (2005)), related to N–S collision (Väisänen et al., 2002; Ehlers et al., 2004) towards the Arc Complex of Central and Western Finland (Korsman et al., 1997). A suture zone separates the Arc Complexes (Fig. 1; Lahtinen, 1996). The collision also involved the Bergslagen area rocks (Lahtinen et al., 2005), which may be correlated with the Uusimaa belt (Allen et al., 1996; Nironen, 1997). The early Svecofennian event was locally associated with partial melting in southern Finland (Hopgood et al., 1983).

Subsequent tectonic evolution involved crustal extension at ~1.86–1.84 Ga (Lahtinen et al., 2005), as revealed by metadiabase dykes cross-cutting early Svecofennian deformation structures (Ehlers et al., 2004),

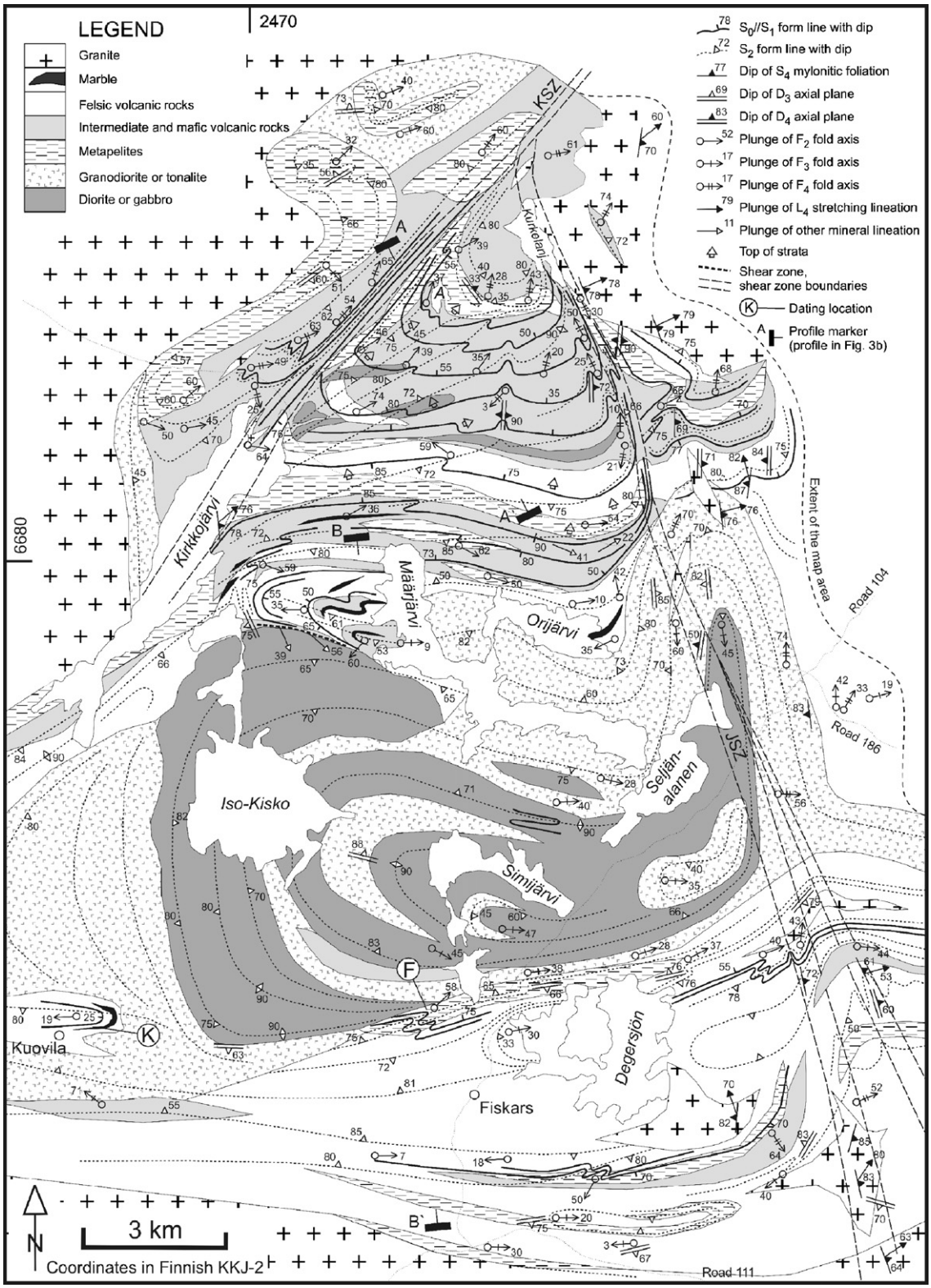


Fig. 2. Geological map of the study area. KSZ = Kisko shear zone, JSZ = Jyly shear zone; dating locations: K = Kuovila, F = Fiskars. Lakes: A = Ahdistonjärvi.

intra-continental sedimentary basin formation (Bergman et al., 2006; Nironen and Lahtinen, 2006) and seismic data (Korja and Heikkinen, 2005). Lahtinen et al. (2005) considered this crustal extension responsible for the heat source for the crustal melting to produce the late Svecofennian granites and migmatites at ~1.84–1.80 Ga (Huhma, 1986; Suominen, 1991; Korsman et al., 1999; Väisänen et al., 2000; Jurvanen et al., 2005; Kurhila et al., 2005; Mouri et al., 2005). Crustal melting was synchronous with a new period of crustal shortening (Väisänen et al., 2002) during a continent-continent collision (the Svecobaltic orogen by Lahtinen et al. (2005)), i.e. the late Svecofennian event (Ehlers et al., 1993), as used in this paper. Metamorphism during the late Svecofennian event was of high-temperature, low-pressure type and it locally reached granulite facies (Schreurs and Westra, 1986; Korsman et al., 1999).

The age of volcanism in southern Finland ranges between 1.90–1.88 Ga (e.g. Patchett and Kouvo, 1986; Vaasjoki, 1994; Reinikainen, 2001; Skyttä et al., 2005). Väisänen and Mänttäri (2002) dated progressive volcanic activity in the Orijärvi area starting at $1895 \pm 2.4$ Ma at the base of the stratigraphy and continuing until $1878 \pm 3.4$ Ma at higher stratigraphic levels. The Uusimaa belt has been interpreted either as a palaeo-island arc (e.g. Hietanen, 1975; Latvalahti, 1979; Gaál, 1990; Ploegsma and Westra, 1990), back-arc basin (e.g. Colley and Westra, 1987; Nironen, 1997) or intra-continental, or continental margin back-arc, extensional region developed on older continental crust (Weihed et al., 2005). The early Svecofennian intrusive phases within the Uusimaa belt include 1.90–1.88 Ga tonalitic-gabbroic suites (Huhma, 1986; Patchett and Kouvo, 1986), which are considered subvolcanic rocks (Väisänen et al., 2002; Ehlers et al., 2004).

The early Svecofennian deformation in the Uusimaa belt resulted in recumbent folds related to thrusting (Van Staal and Williams, 1983; Schreurs and Westra, 1986; Bleeker and Westra, 1987; Ehlers et al., 1993); thrusting towards ESE–SSE was interpreted in the Orijärvi area (Ploegsma and Westra, 1990), whereas the early folds in the western part of the Uusimaa belt, in the Kemiö area, are overturned towards west and northwest (Ehlers et al., 1993; Lindroos and Ehlers, 1994). Axial-planar faults associated with early folds have been found locally (Van Staal and Williams, 1983). The late Svecofennian events transposed the early structures predominantly into upright, east–northeast trending folds. They were associated with thrusting towards northwest and with dextral shearing along east–west trending sub-vertical strike-slip zones, thus defining an overall zone of dextral transpression with approximately SE–NW compression in the late Svecofennian granite–migmatite zone (Ehlers et al., 1993; Lindroos et al., 1996). The strike-slip zones and other sub-vertical shear zones were formed due to deformation partitioning during the late Svecofennian stages (Nironen, 1999; Väisänen and Hölttä, 1999; Torvela and Annersten, 2005). Ploegsma and Westra (1990) suggested that the early structures within the Orijärvi area were preserved due to strain partitioning along the anatectic migmatites that started simultaneously with the late Svecofennian migmatisation.

## 3. Structural data

In our mapping of the Orijärvi area (Fig. 2), we placed particular emphasis upon the development of fabrics, degrees of migmatisation and the presence or absence of late Svecofennian granites or pegmatites. Based on the relative age of deformation, the area was further divided into seven geographical sub-areas (Fig. 3) representing three different structural domains. These include: (a) $D_2$-dominated areas without migmatisation (Kuovila and Orijärvi), (b) $D_2$-dominated areas with $D_3$ overprint (Fiskars and Iso-Kisko), and (c) $D_4$-dominated areas, either directly defined by shear zones (Kisko and Jyly shear zones), or by $D_4$-transposed structures related to the shear zones (Toija). The area on the eastern side of the Jyly shear zone displays characteristic structures of the late Svecofennian granite–migmatite zone where $D_3$ folding, associated with crustal melting, has deformed the sub-horizontal $S_2$ planes into an upright position. Fig. 3 illustrates the sub-area division, stereographic projections of the dominant structural elements in each sub-area and two cross-sections across the study area. The early Svecofennian $D_2$ and the late Svecofennian $D_3$ deformations were both prograde metamorphic, while $D_4$ was retrograde.

### 3.1. Kuovila sub-area

The Kuovila sub-area consists of bimodal volcanic rocks, volcaniclastic conglomerates, banded iron formations, marbles and granodioritic–dioritic–gabbroic intrusives. Primary sedimentary and volcanic structures are well preserved in the area. The main structural feature of the Kuovila sub-area is an upright $D_2$ synform with an axial-planar main fabric ($S_2$; Skyttä et al., 2005). $F_2$ folds deform the bedding planes ($S_0$) and the weak, localised, bedding-parallel $S_1$ foliation, and have curvilinear $F_2$ fold axes, which spread from WSW to ENE. The supracrustal rocks were not migmatised and no pegmatite dykes are found to intrude the supracrustal rocks. Granodioritic dykes, axial-planar to $F_2$ folds and con-

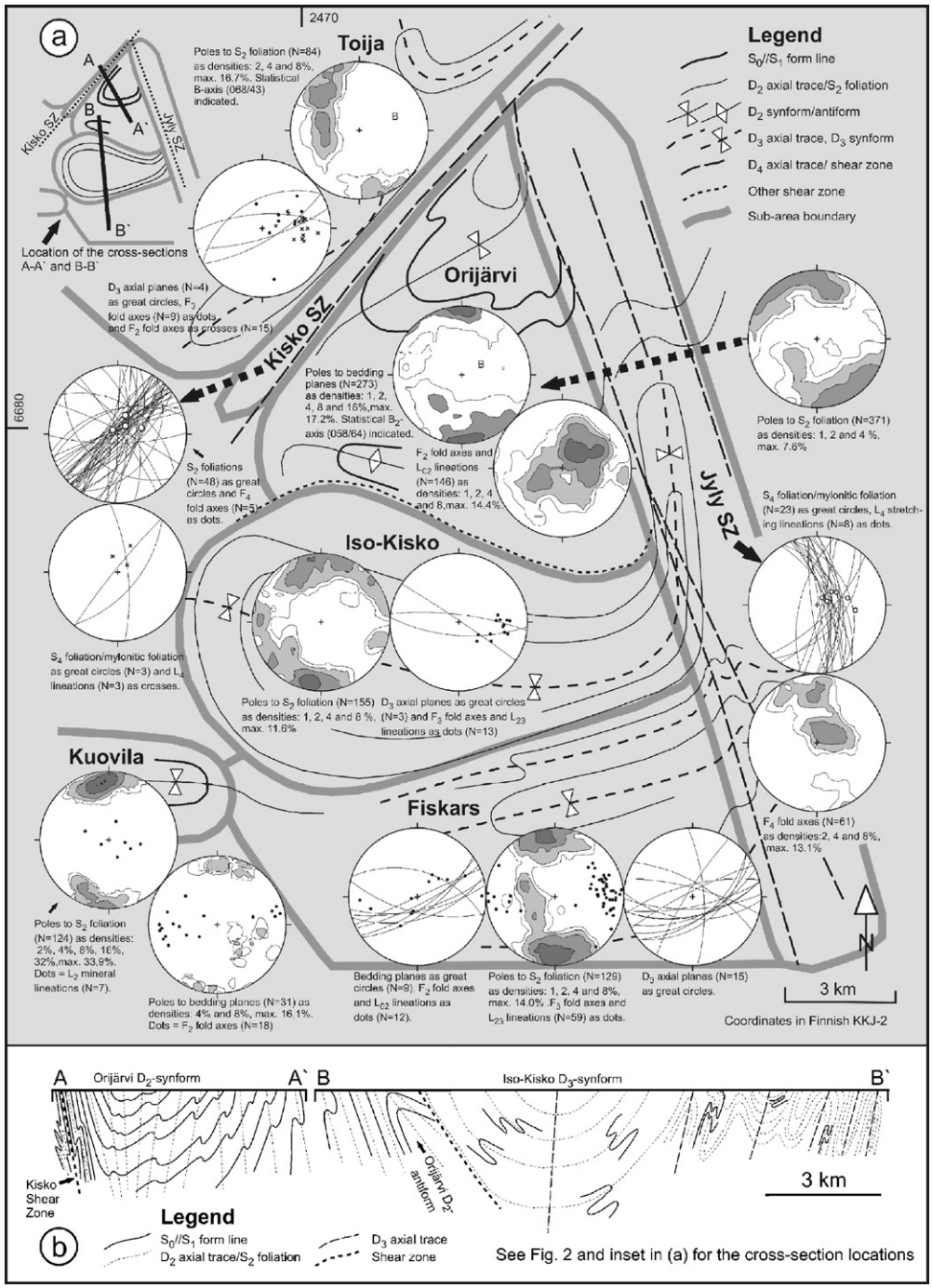


Fig. 3. (a) Sub-area division and related stereographic projections (lower hemisphere, equal-area) showing the main structures within each sub-area. Inset: locations of the cross-sections in (b). Fold axes and the related intersection lineations are merged in the projections from the Fiskars and Orijärvi sub-areas due to their sub-parallelism. (b) Cross-sections A–A′ and B–B′, see inset in (a) and Fig. 2 for the location of cross-sections. The presented data is based on a total number of over 2900 structural measurements from over 1500 localities.

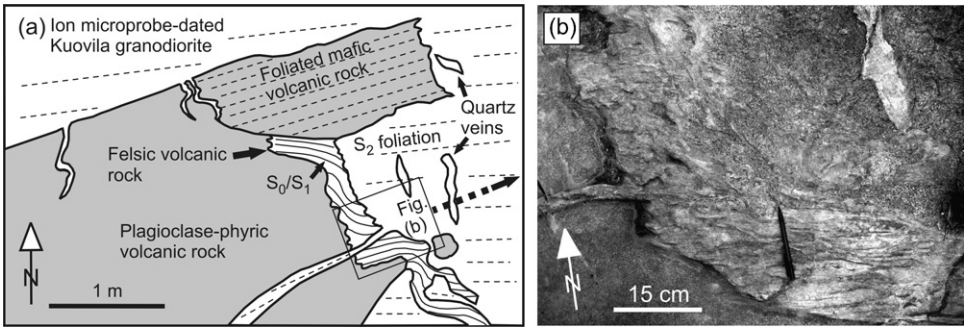


Fig. 4. (a) Line drawing and (b) outcrop photograph illustrating the structural setting of the ion microprobe-dated Kuovila granodiorite, which intruded syntectonically with respect to $D_2$ deformation.

taining $S_2$ are found at the $F_2$ fold hinges (Fig. 4). Therefore, we interpret the granodiorite as syntectonic with respect to $D_2$. Ion microprobe U–Pb dating results of the granodiorite are presented in Section 4.

### 3.2. Orijärvi sub-area

Well-preserved volcanic and sedimentary primary structures (bedding, graded bedding, load casts, laminar beds, pillow lavas, concretions) are common within the Orijärvi sub-area. The rocks include volcanic and sedimentary rocks, mafic and felsic dykes, and granodiorites, tonalites and gabbros. $D_1$ structures have not been found, but $S_1$ foliation, sub-parallel to $S_0$, occurs in the mica-rich metasediments and may be related to thrusting during $D_1$ (Skyttä et al., 2005). The $D_2$-folded supracrustal rocks in the northern part of the area define an upright, gently NE-plunging $D_2$ synform (Orijärvi synform), whereas the southern part of the area forms a steeply south-dipping, west-plunging $D_2$ antiform (Orijärvi antiform). Metre-scale open to tight $F_2$ folds deform the bedding planes and the generally weakly developed $S_1$ foliations, and are associated with penetrative axial-planar $S_2$ foliation, the main foliation in the Orijärvi sub-area. A moderately south-dipping high-strain zone with SE-plunging mineral lineations is located along the southern contact of the Orijärvi sub-area and therefore separates the $D_2$-dominated areas in the north from the $D_3$-affected areas in the south. The movement sense along the high-strain zone is not known, but the lower-grade rocks to the north, and the orientation of the lineations suggest reverse dextral oblique shearing.

Metapelitic layers along the Orijärvi synform contain abundant andalusite and cordierite porphyroblasts and some fibrolitic sillimanites. Andalusites (And) are present as at least two generations and they commonly contain inclusion trails of matrix foliations: (1) The first generation ($And_1$) grew during $D_2$, as revealed by slightly curved $S_1$ inclusion trails within the blasts (Fig. 5a, on the southern limb of the Orijärvi synform). (2) The second generation ($And_2$) overgrew $S_2$ foliation, mainly on the mica-rich $D_2$ strain-caps at the edges of $And_1$. Late-$D_2$ to post-$D_2$ growth is evident, as $S_2$ foliation shows no deflection at the contacts of $And_2$ (Fig. 5a). A similar succession may be observed along the NW limb of the Orijärvi synform, where the $S_1$ foliation traces within $And_1$ are folded, and the straight $S_2$ foliation traces are at right angles to $S_1$ (Fig. 5b). Cordierite overgrew $S_2$ foliation and fibrolitic sillimanite replaced andalusite at the grain margins, e.g. along the contacts between two $And_2$ grains (Fig. 5a). Chlorite and muscovite grew both post-tectonic with respect

Fig. 5. Detailed structures in the Orijärvi sub-area. (a) The first generation of andalusite porphyroblasts grew syn-$D_2$ ($And_1$), while the second generation of andalusites ($And_2$) grew over $S_2$ foliation, indicated by straight $S_2$ foliation showing no deflection at the $And_2$ contacts. Sillimanite replaces $And_2$ grains at the margins between two $And_2$ grains. Photomicrograph, plane-polarised light. Southern limb of the Orijärvi $D_2$ synform. (b) Folded inclusion trails of $S_1$ in the central part of the andalusite porphyroblast ($And_1$) and straight $S_2$ inclusion trails at the margins ($And_2$). Photomicrograph, cross-polarised light. NW limb of the Orijärvi $D_2$ synform, SW of lake Ahdistonjärvi. (c) Graded bedding indicating top of the strata towards north and NE-vergent $S_2$ foliation cross-cutting the bedding planes. Southern limb of the Orijärvi D2 synform. (d) Graded bedding indicating top of the strata towards ESE. The bedding planes show sinistral $F_2$ folds with axial-planar $S_2$ foliation. Along the NW limb of the Orijärvi $D_2$ synform, near lake Ahdistonjärvi. (e) Open $D_2$ folding of the bedding with subvertical axial planar $S_2$ foliation in the hinge of the Orijärvi $D_2$ synform, SW of lake Ahdistonjärvi. Oblique section. (f) Deformed conglomerate with sub-elliptical markers. *YZ*-plane on the left and *XZ*-plane on the right. (g) Line drawing of a west-vergent $F_3$ or $F_4$ fold deforming $S_2$ foliation planes. The pegmatite dyke likely intruded during $D_3$ or $D_4$. Vertical section.

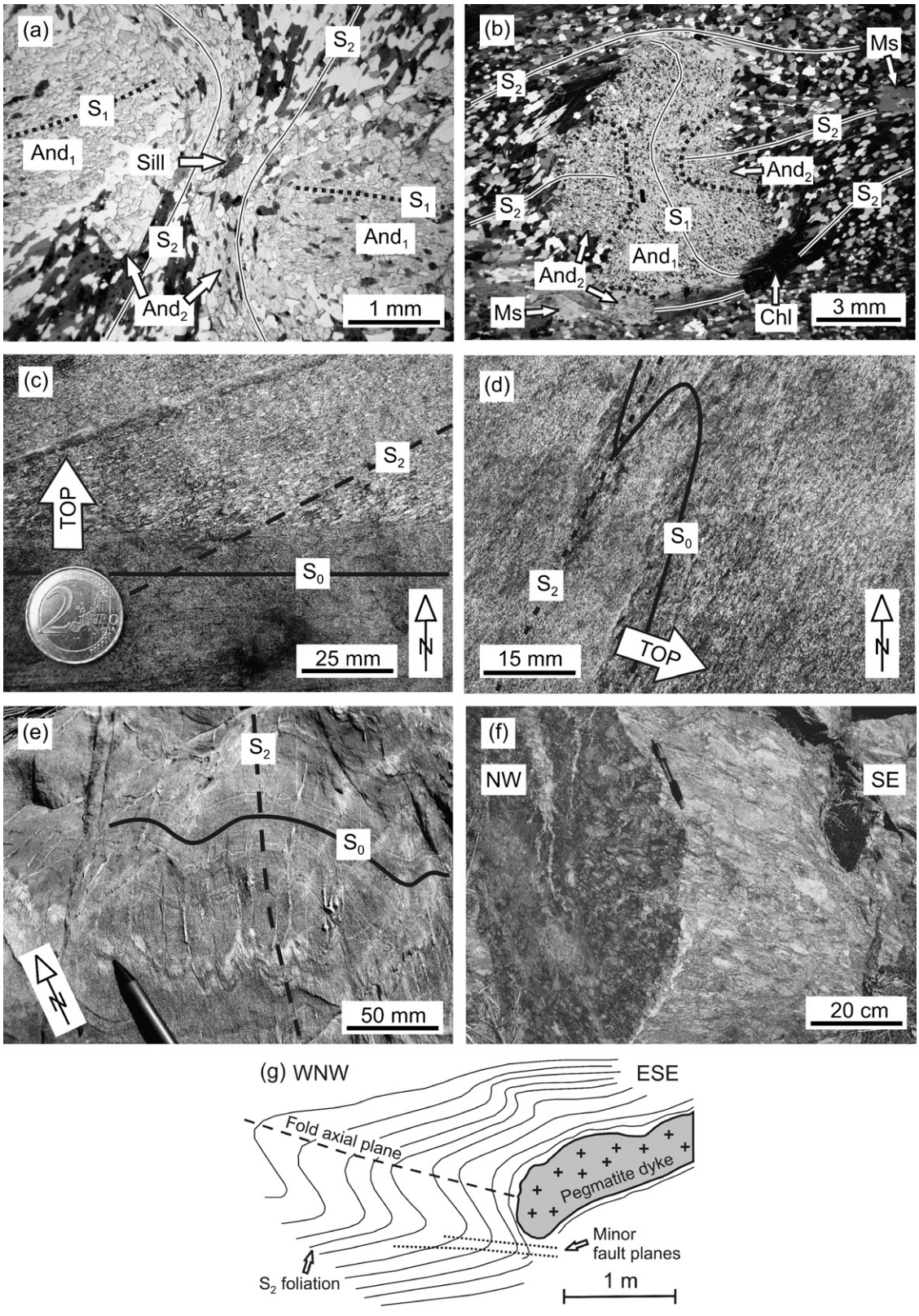
(a)
S2
S1
And1
Sill
S1
S2
And1
And2
1 mm
(b)
Ms
S2
S2
And2
S2
S2
S1
And1
And2
Ms
Chl
3 mm
(c)
S2
TOP
S0
25 mm
N
(d)
S0
S2
15 mm
TOP
N
(e)
S2
S0
N
50 mm
(f)
NW
SE
20 cm
(g) WNW
ESE
Fold axial plane
Pegmatite dyke
Minor
fault planes
S2 foliation
1 m

to $D_2$ and syntectonic with the later stages of progressive deformation ($D_4$) in the shear zones. We conclude that lower amphibolite facies metamorphic conditions within the andalusite stability field across the Orijärvi $D_2$ synform–antiform pair were prevailing during $D_2$ (this study; Eskola, 1914) and the sillimanite stability field conditions were prevailing during $D_3$. $D_3$ did not involve partial melting in the Orijärvi sub-area. The peak temperature has been estimated at 600 °C (Schumacher and Czank, 1987; Schneiderman and Tracy, 1991).

Stratigraphic facing directions determined from graded metagraywackes consistently indicate younging towards north along the southern limb of the Orijärvi synform (Fig. 5c), towards NE in the hinge of the synform and towards east on the western limb of the synform (Fig. 5d), thus defining the structure as a NE-facing $D_2$ syncline. For clarity, we refer to this structure as a $D_2$ synform. Further evidence for the large-scale $F_2$ fold within the Orijärvi sub-area is evident as the $S_2$ foliation vergences are opposite on the southern and western limbs (Figs. 2, 5c and d) and $S_2$ occurs at right angles to the gently dipping $S_0$ in the hinge of the fold (Fig. 5e). Parasitic $F_2$ folds of decimetre- to metre-scale are mainly found along the southern limb of the synform, whereas the Kisko shear zone largely cuts the western limb, partly removing the lithological marker horizons such as graded metagraywacke, conglomerate and metapelite along the synform. Stratigraphic facing directions could not be measured on the southern limb of the Orijärvi antiform.

Constrictional deformation took place along the southern limb of the Orijärvi synform, defined by prolate fragment shapes within deformed conglomerate (Fig. 5f). Other locations along the southern limb of the synform with less strained conglomerate indicate strain localisation into specific horizons.

The post-$D_2$ deformation structures within the Orijärvi synform are mainly rare dextral asymmetric $F_3$ drag-folds with sub-vertical axes. On the southern limb of the Orijärvi antiform, $S_2$ is deformed into open north-vergent asymmetric $F_3$ folds. The $D_3$ and $D_4$ structures become more abundant towards the Kisko and Jyly shear zones. Ductile shear bands and apparent sinistral rotation of the older structures into the shear zones are found when approaching both the Jyly and Kisko shear zones. At the northernmost part of the Orijärvi synform, east of lake Ahdistonjärvi, overturned west-vergent $F_3$ or $F_4$ folds, associated with pegmatite dykes filling the fold hinges, deform the $S_2$ planes (Fig. 5g). $S_2$ planes are strongly curved also on the map scale in the northern apex of the Orijärvi triangle, i.e. in the vicinity of the intersecting shear zones (Fig. 2).

### 3.3. Fiskars sub-area

The Fiskars sub-area in the southern part of the study area consists mainly of felsic volcanic-sedimentary rocks intercalated with intermediate to mafic volcanic layers and few metapelitic layers. The metapelites display thin quartz-rich leucosome veins. The supracrustal rocks were intruded by intermediate dykes and later by granitic dykes. The earliest folds are tight to isoclinal $F_2$ folds, which presently have steep axial planes. $F_2$ fold axes plunge moderately to steeply towards ENE and SW. The mainly $S_1$-parallel quartz-rich leucosomes were folded together with intense $S_1$ foliation, but in places they occur along $D_2$ axial planes (Fig. 6a). This indicates that migmatisation started during $D_1$ or early $D_2$ and continued during $D_2$. In contrast to the metapelitic rocks, the main fabric of the quartz-feldspar rich rocks is $S_2$, while the bedding planes and the weaker layer-parallel $S_1$ were folded (Fig. 6b).

Dykes on intermediate compositions have intruded the supracrustal rocks along $F_2$ axial planes (Fig. 6c and d). These dykes exhibit penetrative foliation parallel to $S_2$ in the supracrustal rocks and therefore indicate syn-$D_2$ origin for the dykes. One such dyke has been dated with ion microprobe by U–Pb system on zircons and the results will be presented in Section 4. Upright $F_3$ folds with gently plunging fold axes refold the previous structures and are associated with patchy granitic leucosomes and axial-planar pegmatite dykes, indicating that peak metamorphic conditions prevailed during $D_3$ (Fig. 6e and f). $D_3$ axial surfaces generally trend east–west, but towards east they show apparent counter-clockwise rotation towards parallelism with the Jyly shear zone. Intensity of the $D_3$ folding increases towards the contact of the late Svecofennian granite-dominated area in the south. Sub-horizontal $S_2$ foliation planes are observed in the SE part of the area and at least in one locality they comprise

Fig. 6. Detailed structures in the Fiskars and Iso-Kisko sub-areas. (a) Tight to isoclinal $F_2$ folds associated with syn-$D_1$ or early $D_2$ layer-parallel (on the left) and syn-$D_2$ or late-$D_2$ axial-planar (under the text box in the centre) quartz-rich leucosomes. Note the intense $S_1$ foliation, while $S_2$ was only locally developed in the $F_2$ hinges. (b) Low-strain $F_2$ folds with axial-planar main foliation, $S_2$. Photomicrograph, plane-polarised light. (c) Line drawing and (d) outcrop photograph illustrating the structural setting of the ion microprobe-dated Fiskars intermediate syn-$D_2$ dyke. (e) Line drawing and (f) outcrop photograph of open $F_3$ folding associated with syntectonic patchy granitic leucosomes. Note the intrafolial $F_2$ folds in (e).

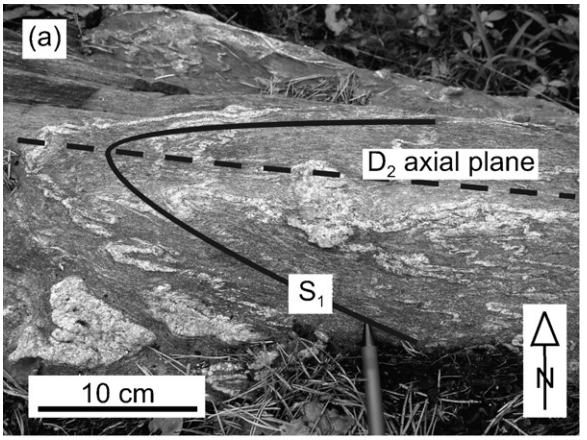
(a)
D2 axial plane
S1
10 cm
N

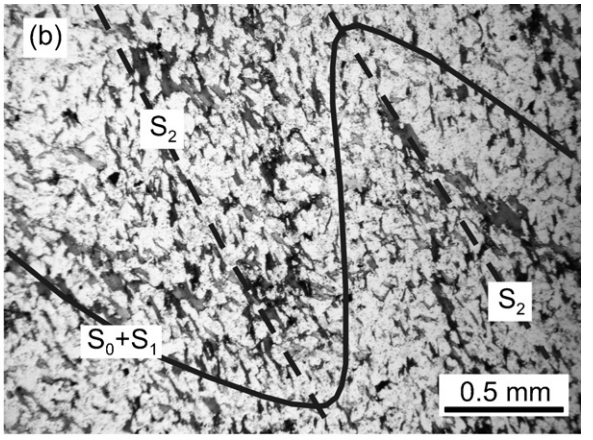
(b)
S2
S2
S0+S1
0.5 mm

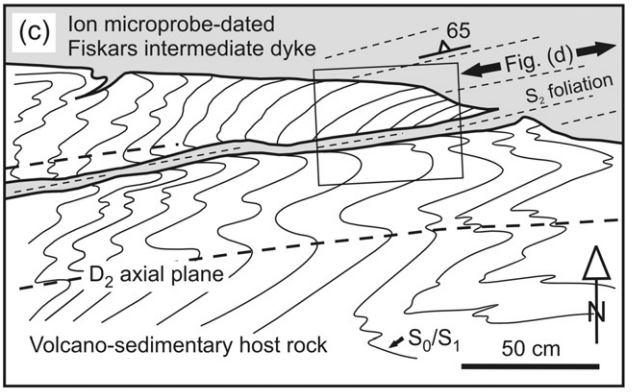
(c)
Ion microprobe-dated
Fiskars intermediate dyke
65
Fig. (d)
S2 foliation
D2 axial plane
Volcano-sedimentary host rock
S0/S1
50 cm
N

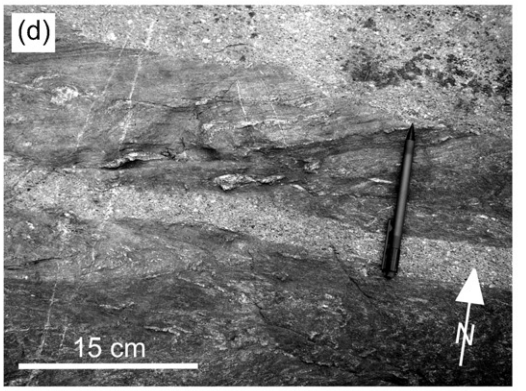
(d)
15 cm
N

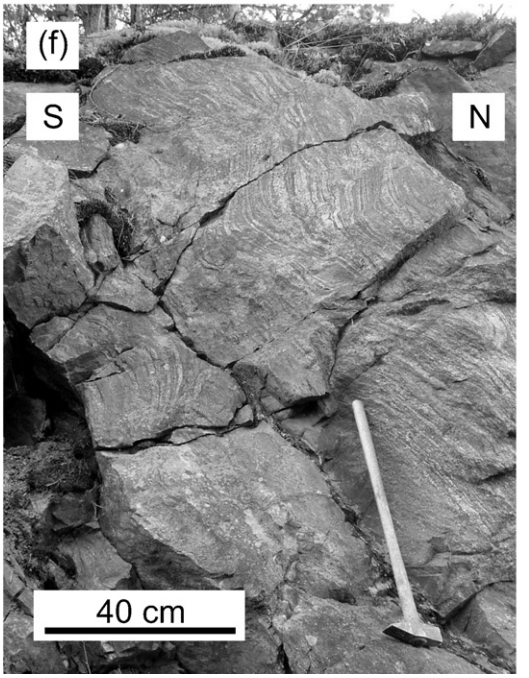
(f)
S
N
40 cm

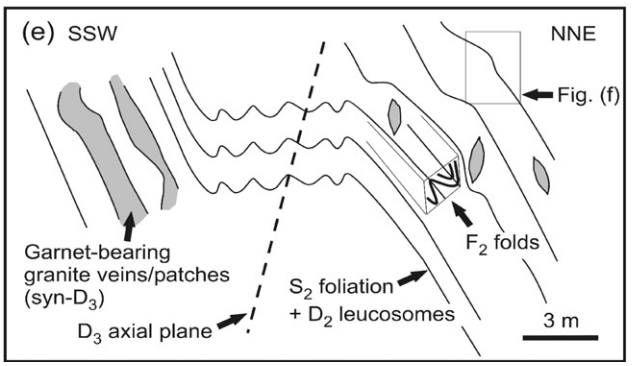
(e) SSW
NNE
Fig. (f)
F2 folds
Garnet-bearing
granite veins/patches
(syn-D3)
D3 axial plane
S2 foliation
+ D2 leucosomes
3 m

a conform granite with a gently dipping foliation. Few occurrences of boudinaged $S_2$ foliations, associated with ptygmatically folded granitic leucosome veins, indicate apparent vertical shortening in the areas where the $S_2$ foliation is sub-horizontal.

### 3.4. Iso-Kisko sub-area

The Iso-Kisko sub-area consists of plutonic rocks with compositions ranging from tonalite to gabbro. Väisänen et al. (2002) consider that these ~1.90 Ga rocks are magma chambers to the volcanic rocks in the area. The main structure is a kilometre-scale tight $F_3$ fold that deforms and folds the main foliation ($S_2$) visible in the plutonic rocks. K-feldspar rich pegmatite dykes, axial-planar to $F_3$ folds occur in the $F_3$ fold hinge. Relics of $F_2$ folds, associated with axial-planar $S_2$ foliations, deforming the compositional layering ($S_0/S_1$) are locally found. The plutonic rocks define a doubly plunging synform with vertical to steep $S_2$ foliations in the western hinge of the $F_3$ fold, moderately east-dipping $S_2$ towards east, and SW-dipping $S_2$ in the eastern part of the synform. The Jyly shear zone in the east later reoriented the originally east–westerly $F_3$ synform. The reorientation produced the basin, which is a $D_3/D_4$ interference structure.

### 3.5. Jyly and Kisko shear zone sub-areas

$D_4$ strain was partitioned into two ductile high-strain zones, the Jyly shear zone (JSZ) and the Kisko shear zone (KSZ). The JSZ trends NNW–SSE as an at least 50 km long high-strain zone across the Uusimaa belt and separates the syn-$D_3$ migmatites in the east and the predominantly well-preserved, non-migmatitic rocks in the west. The NNE-trending KSZ truncates the JSZ along the NW limb of the Orijärvi $D_2$ synform. Both shear zones express strain partitioning into less-intense retrograde $F_4$-folded areas at the margins and into more intense mylonitic zones in the core of the shear zones. Both the folding and the mylonitisation deformed the pegmatites, which are absent in the early Svecofennian deformations, thus constraining the relative timing of shear zone deformation as syn-$D_3$ or post-$D_3$. The absence of good outcrop-scale $F_3/F_4$ interference patterns combined with map-scale refolding of the $D_3$ axial surfaces along the shear zones (Fig. 2) favours post-$D_3$ age for the deformation. Therefore, all the folds in the KSZ and JSZ sub-areas are here treated as $D_4$ structures (see discussion e.g. in Carreras et al. (2005)). Brittle overprint on the ductile $D_4$ deformation as well as hydrothermal alteration associated with shearing are locally observed especially within the KSZ.

The JSZ sub-area consists of several parallel steeply ENE-dipping ductile $D_4$ shear zones, which have steep east-plunging stretching lineations and show reverse east-block-up movements, recorded by asymmetric kinematic indicators ($\sigma$- and $\delta$-clasts, secondary oblique foliations of recrystallised quartz grains, mica fish, shear bands, cf. Passchier and Trouw, 1996) in mylonitic pegmatites (Fig. 7a) both in the field and in microscopic-scale. Shear strain across the mylonite zones is heterogeneously distributed, recorded by a range of suites from protomylonites to well-developed ultramylonites. Opposite relative movement senses have been observed locally. Low-temperature overprint and cataclastic faults most probably indicate later reactivation of the shear zone as shown by the Rb–Sr age of $1533 \pm 23$ Ma on ultramylonites along the northern continuation of the KSZ (Ploegsma, 1989).

Retrograde $F_4$ folds occur both at the margins and between the parallel mylonite zones. $F_4$ fold axes are generally highly curvilinear. Depending on the $D_4$ strain intensity and the mineral composition of the host rock, retrograde $S_4$ foliation is either the main foliation of the rocks within the JSZ, such as with the $F_2$-folded, non-migmatitic, mica-poor felsic volcanic rocks, whereas $S_4$ has not developed in the mica-rich rocks. The majority of the $F_4$ folds are upright and show apparent left-lateral deflection of the pre-existing structures into the shear zone. Some $F_4$ folds within the Orijärvi synform are overturned towards west, as described in Section 3.2.

Mylonites deforming the late Svecofennian pegmatites within the KSZ sub-area show east-side-up movements. Stretching lineations and the axes of the KSZ-related folds are sub-parallel, but generally steeper than the $F_2$ fold axes within the Orijärvi sub-area. Kink/chevron style folds that deformed $S_2$ foliation planes are common on the western margin of the KSZ. The associated structures include fractures, faults (Fig. 7b) and spaced $S_4$ foliations. These indicate that deformation post-dates the metamorphic peak. Most $D_4$ faults indicate apparent left-lateral movement on horizontal surfaces, as also do the rarely observed decametre-scale ductile S/C shear bands.

### 3.6. Toija sub-area

The Toija sub-area consists of migmatised metapelites and picritic and basaltic lavas with pillow structures. In the southern part of the sub-area $F_2$ fold axes plunge to the east but towards north they are rotated towards parallelism with the linear fabrics within the KSZ. The pillow lavas occurring in the hinge zone of a large-scale $F_3$ fold indicate local

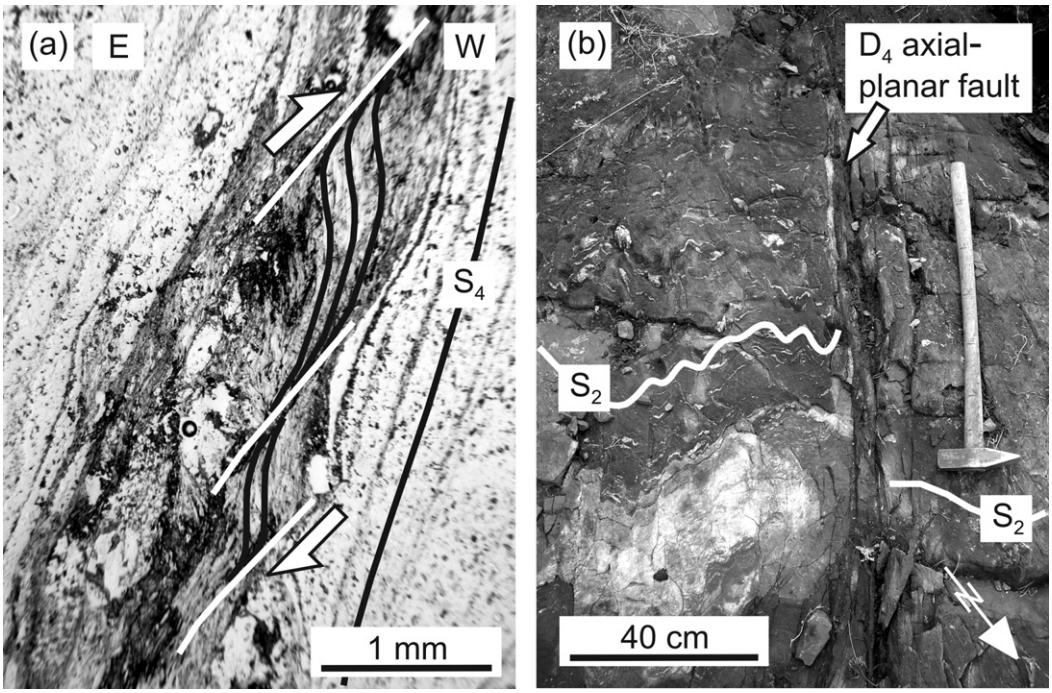


Fig. 7. Detailed structures in the Jyly and Kisko shear zone sub-areas. (a) A micaceous domain within a mylonitised pegmatite in the Jyly shear zone displaying C′-type shear bands. East-block-up shear sense. Photomicrograph, plane-polarised light. Vertical section. (b) $D_4$ axial-planar faults in the margin of the Kisko shear zone.

pre-$D_2$ or syn-$D_2$ flattening, revealed by high-strain zones parallel to $S_2$ foliation planes that are at right angles both to the $D_3$ axial surfaces and to the KSZ. Restoring of the primary geometry of the Toija sub-area is hampered by multiple deformations along the KSZ, thus making regional correlation of the structural succession difficult. The main deformation was, however, syntectonic with the migmatisation, and may thus be correlated with $D_3$ in the other parts of the study area.

## 4. Age of $D_2$ deformation

In order to date the early deformation, two rock samples were taken for zircon ion microprobe U–Pb dating. Both the Kuovila granodiorite sample and the Fiskars intermediate dyke sample are syntectonic with respect to $D_2$ folding, as described in Sections 3.1 and 3.3.

### 4.1. Analytical methods

The selected zircons for the ion microprobe U–Pb dating were mounted in epoxy, polished and coated with gold. The ion microprobe U–Pb analyses were made using the Nordic SIMS (NordSIM) Cameca IMS 1270 instrument at the Swedish Museum of Natural History, Stockholm, Sweden. The spot-diameter for the 9 nA primary $O_2^-$ ion beam was ~25 μm. Oxygen flooding in the sample chamber was used to increase the production of $Pb^+$ ions. Three counting blocks, each including four cycles of the Zr, Pb, Th, and U species of interest were measured from each spot. The mass resolution ($M/\Delta M$) was 5400 (10%). The raw data were calibrated against a zircon standard (91 500; Wiedenbeck et al., 1995) and corrected for modern common lead ($T=0$; Stacey and Kramers, 1975). For the detailed analytical procedure see Whitehouse et al. (1997,1999). Plotting of the U–Pb isotopic data and the age calculations were done using the Isoplot/Ex 3 program (Ludwig, 2003). The data-point error ellipses in the concordia diagrams are 2 sigma. All errors in age results are 2 sigma errors with decay constant errors ignored.

### 4.2. Kuovila granodiorite (n1806)

The Kuovila granodiorite sample yielded a large amount of mainly brown, prismatic, translucent to transparent magmatic zircon. The population looks quite homogeneous when ignoring a few pale-coloured, long prismatic, and transparent zircons. In the BSE (back scattered electron) images, the zircons show either very weak zoning or are internally rather homogeneous (Fig. 8). The

Table 1
Zircon ion microprobe U–Pb isotopic data for Kuovila granodiorite and Fiskars intermediate dyke

| Sample/spot# | Internal structure of dated zircon domain | Derived ages (Ma) | | | | | | Corrected ratios | | | | | | | | | | | | | |
|---|---|---|---|---|---|---|---|---|---|---|---|---|---|---|---|---|---|---|---|---|---|
| | | $^{207}Pb/^{206}Pb$ | ±σ | $^{207}Pb/^{235}U$ | ±σ | $^{206}Pb/^{238}U$ | ±σ | $^{207}Pb/^{206}Pb$ | ±σ (%) | $^{207}Pb/^{235}U$ | ±σ (%) | $^{206}Pb/^{238}U$ | ±σ (%) | $r$[a] | Disc. (%)[b] | [U] (ppm) | [Th] (ppm) | [Pb] ppm | $f_{206}$ (%)[c] | Th/U calc. | $^{206}Pb/^{204}Pb$ measured |
| Kuovila granodiorite (*n*1806) | | | | | | | | | | | | | | | | | | | | | |
| *n*1806—01a | Weakly zoned | 1875 | 5 | 1869 | 11 | 1864 | 21 | 0.1147 | 0.3 | 5.301 | 1.3 | 0.3353 | 1.3 | 0.98 | | 809 | 302 | 332 | {0.00} | 0.37 | 4.26E+05 |
| *n*1806—02a | Quite homogeneous | 1859 | 6 | 1849 | 12 | 1840 | 21 | 0.1137 | 0.3 | 5.181 | 1.3 | 0.3304 | 1.3 | 0.97 | | 564 | 139 | 221 | 0.25 | 0.24 | 7.43E+03 |
| *n*1806—03a | Weakly zoned | 1880 | 5 | 1874 | 12 | 1868 | 21 | 0.1150 | 0.3 | 5.330 | 1.3 | 0.3361 | 1.3 | 0.97 | | 663 | 218 | 270 | 0.01 | 0.33 | 1.95E+05 |
| *n*1806—04a | Weakly zoned | 1868 | 6 | 1865 | 12 | 1862 | 21 | 0.1142 | 0.3 | 5.275 | 1.4 | 0.3349 | 1.3 | 0.97 | | 346 | 145 | 143 | 0.06 | 0.41 | 3.14E+04 |
| *n*1806—05a | Weakly zoned | 1881 | 4 | 1889 | 12 | 1897 | 22 | 0.1151 | 0.2 | 5.429 | 1.3 | 0.3422 | 1.3 | 0.98 | | 988 | 393 | 415 | 0.01 | 0.40 | 2.90E+05 |
| *n*1806—07a | Zoned | 1880 | 5 | 1887 | 12 | 1894 | 22 | 0.1150 | 0.3 | 5.415 | 1.3 | 0.3416 | 1.3 | 0.98 | | 700 | 175 | 284 | {0.00} | 0.25 | 3.86E+05 |
| *n*1806—08a | Zoned | 1868 | 4 | 1902 | 11 | 1933 | 22 | 0.1142 | 0.2 | 5.506 | 1.3 | 0.3496 | 1.3 | 0.99 | 1.1 | 781 | 168 | 321 | {0.00} | 0.22 | 4.33E+05 |
| *n*1806—09a | Zoned inner domain | 1871 | 6 | 1961 | 12 | 2048 | 23 | 0.1144 | 0.3 | 5.899 | 1.4 | 0.3739 | 1.3 | 0.97 | 7.7 | 486 | 90 | 212 | 0.62 | 0.20 | 3.01E+03 |
| *n*1806—09b | Homogeneous rim domain | 1874 | 3 | 1889 | 11 | 1902 | 22 | 0.1146 | 0.2 | 5.424 | 1.3 | 0.3431 | 1.3 | 0.99 | | 1498 | 250 | 597 | 0.07 | 0.17 | 2.64E+04 |
| *n*1806—10a | Weakly zoned | 1878 | 5 | 1876 | 11 | 1875 | 21 | 0.1149 | 0.3 | 5.347 | 1.3 | 0.3375 | 1.3 | 0.98 | | 626 | 140 | 249 | 0.02 | 0.23 | 1.21E+05 |
| *n*1806—12a | Quite homogeneous, long | 1876 | 5 | 1857 | 12 | 1840 | 21 | 0.1148 | 0.3 | 5.227 | 1.3 | 0.3304 | 1.3 | 0.97 | | 652 | 155 | 256 | 0.51 | 0.25 | 3.69E+03 |
| *n*1806—13a | Zoned, long | 1880 | 5 | 1882 | 11 | 1884 | 21 | 0.1150 | 0.3 | 5.383 | 1.3 | 0.3395 | 1.3 | 0.98 | | 955 | 452 | 405 | 0.03 | 0.47 | 6.15E+04 |
| *n*1806—14a | Zoned, long | 1877 | 5 | 1882 | 12 | 1887 | 21 | 0.1148 | 0.3 | 5.384 | 1.3 | 0.3400 | 1.3 | 0.98 | | 666 | 234 | 276 | 0.14 | 0.36 | 1.29E+04 |
| *n*1806—15a | Zoned, long | 1884 | 13 | 1884 | 13 | 1884 | 22 | 0.1153 | 0.8 | 5.396 | 1.5 | 0.3395 | 1.3 | 0.87 | | 935 | 394 | 394 | 0.54 | 0.44 | 3.47E+03 |
| *n*1806—16a | Homogeneous inner domain | 1883 | 10 | 1769 | 12 | 1673 | 19 | 0.1152 | 0.5 | 4.708 | 1.4 | 0.2964 | 1.3 | 0.93 | −9.3 | 1460 | 565 | 517 | 1.89 | 0.24 | 9.92E+02 |
| *n*1806—17a | Quite homogeneous | 1874 | 7 | 1832 | 12 | 1795 | 21 | 0.1146 | 0.4 | 5.075 | 1.4 | 0.3212 | 1.3 | 0.96 | −1.7 | 484 | 151 | 186 | 0.81 | 0.26 | 2.31E+03 |
| *n*1806—18a | Zoned | 1888 | 16 | 1893 | 14 | 1899 | 22 | 0.1155 | 0.9 | 5.455 | 1.6 | 0.3425 | 1.3 | 0.82 | | 611 | 218 | 254 | 1.7 | 0.33 | 1.10E+03 |
| *n*1806—19a | Quite homogeneous, long | 1873 | 7 | 1829 | 12 | 1791 | 21 | 0.1145 | 0.4 | 5.060 | 1.4 | 0.3204 | 1.3 | 0.96 | −2.0 | 365 | 82 | 138 | 0.19 | 0.21 | 9.68E+03 |
| *n*1806—20a | Quite homogeneous, long | 1889 | 5 | 1903 | 12 | 1916 | 22 | 0.1156 | 0.3 | 5.514 | 1.3 | 0.3461 | 1.3 | 0.98 | | 777 | 337 | 333 | 0.01 | 0.43 | 2.11E+05 |
| Fiskars intermediate dyke (*n*1807) | | | | | | | | | | | | | | | | | | | | | |
| *n*1807—01a | Zoned | 1895 | 8 | 1883 | 12 | 1873 | 22 | 0.1160 | 0.4 | 5.390 | 1.4 | 0.3371 | 1.3 | 0.95 | | 259 | 106 | 108 | 0.16 | 0.41 | 1.18E+04 |
| *n*1807—02a | Zoned | 1870 | 6 | 1885 | 12 | 1898 | 22 | 0.1144 | 0.4 | 5.399 | 1.4 | 0.3424 | 1.3 | 0.96 | | 628 | 397 | 279 | 0.01 | 0.64 | 1.32E+05 |
| *n*1807—03a | Zoned | 1891 | 9 | 1861 | 12 | 1834 | 21 | 0.1157 | 0.5 | 5.249 | 1.4 | 0.3291 | 1.3 | 0.93 | | 351 | 106 | 140 | 0.32 | 0.32 | 5.85E+03 |
| *n*1807—04a | Zoned | 1878 | 6 | 1856 | 12 | 1837 | 21 | 0.1149 | 0.3 | 5.221 | 1.3 | 0.3296 | 1.3 | 0.97 | | 456 | 159 | 183 | 0.02 | 0.35 | 9.07E+04 |
| *n*1807—05a | Zoned core (altered and homogenised rim domain) | 1872 | 5 | 1867 | 12 | 1863 | 21 | 0.1145 | 0.3 | 5.290 | 1.3 | 0.3350 | 1.3 | 0.97 | | 505 | 192 | 207 | 0.09 | 0.39 | 2.19E+04 |
| *n*1807—06a | Zoned | 1871 | 7 | 1888 | 12 | 1903 | 22 | 0.1145 | 0.4 | 5.421 | 1.4 | 0.3435 | 1.3 | 0.96 | | 360 | 112 | 149 | 0.07 | 0.32 | 2.73E+04 |
| *n*1807—07a | Zoned | 1880 | 5 | 1868 | 11 | 1858 | 21 | 0.1150 | 0.3 | 5.297 | 1.3 | 0.3341 | 1.3 | 0.98 | | 534 | 348 | 231 | 0.01 | 0.61 | 1.43E+05 |
| *n*1807—08a | Zoned | 1879 | 6 | 1875 | 12 | 1872 | 21 | 0.1149 | 0.3 | 5.341 | 1.4 | 0.3370 | 1.3 | 0.97 | | 517 | 291 | 222 | 0.24 | 0.55 | 7.93E+03 |
| *n*1807—09a | Zoned | 1848 | 8 | 1868 | 12 | 1887 | 21 | 0.1130 | 0.4 | 5.296 | 1.4 | 0.3400 | 1.3 | 0.95 | | 344 | 112 | 140 | 0.4 | 0.31 | 4.73E+03 |
| *n*1807—10a | Homogenised core | 1875 | 3 | 1904 | 11 | 1931 | 22 | 0.1147 | 0.1 | 5.524 | 1.3 | 0.3492 | 1.3 | 0.99 | 0.6 | 3497 | 4271 | 1781 | 0 | 1.23 | 4.48E+05 |
| *n*1807—11a | Homogenised core | 1878 | 3 | 1890 | 11 | 1901 | 22 | 0.1149 | 0.2 | 5.433 | 1.3 | 0.3431 | 1.3 | 0.99 | | 2048 | 1871 | 968 | 0 | 0.93 | 4.64E+05 |

Table 1 (*Continued*)

| Sample/spot# | Internal structure of dated zircon domain | Derived ages (Ma) | | | | | | Corrected ratios | | | | | | | | | | | | | |
|---|---|---|---|---|---|---|---|---|---|---|---|---|---|---|---|---|---|---|---|---|---|
| | | $^{207}Pb/^{206}Pb$ | ±σ | $^{207}Pb/^{235}U$ | ±σ | $^{206}Pb/^{238}U$ | ±σ | $^{207}Pb/^{206}Pb$ | ±σ (%) | $^{207}Pb/^{235}U$ | ±σ (%) | $^{206}Pb/^{238}U$ | ±σ (%) | r[a] | Disc. (%)[b] | [U] (ppm) | [Th] (ppm) | [Pb] ppm | $f_{206}$ (%)[c] | Th/U calc. | $^{206}Pb/^{204}Pb$ measured |
| *n*1807—12a | Zoned | 1877 | 8 | 1863 | 12 | 1852 | 21 | 0.1148 | 0.5 | 5.267 | 1.4 | 0.3327 | 1.3 | 0.95 | | 237 | 68 | 94 | 0.32 | 0.28 | 5.79E+03 |
| *n*1807—13a | Zoned | 1864 | 7 | 1873 | 12 | 1881 | 21 | 0.1140 | 0.4 | 5.325 | 1.4 | 0.3388 | 1.3 | 0.96 | | 382 | 106 | 154 | 0.06 | 0.27 | 3.14E+04 |
| *n*1807—14a | Zoned | 1878 | 7 | 1882 | 12 | 1885 | 22 | 0.1149 | 0.4 | 5.380 | 1.4 | 0.3396 | 1.3 | 0.96 | | 291 | 85 | 118 | {0.01} | 0.29 | 1.30E+05 |
| *n*1807—15a | Zoned | 1888 | 7 | 1849 | 12 | 1814 | 21 | 0.1155 | 0.4 | 5.176 | 1.4 | 0.3250 | 1.3 | 0.96 | −1.5 | 353 | 102 | 137 | 0.26 | 0.27 | 7.26E+03 |
| *n*1807—16a | Zoned, long | 1878 | 7 | 1870 | 12 | 1864 | 21 | 0.1149 | 0.4 | 5.308 | 1.4 | 0.3352 | 1.3 | 0.96 | | 294 | 107 | 120 | 0.09 | 0.36 | 2.00E+04 |
| *n*1807—17a | Zoned, long | 1886 | 11 | 1876 | 13 | 1867 | 22 | 0.1154 | 0.6 | 5.345 | 1.5 | 0.3359 | 1.3 | 0.91 | | 130 | 33 | 52 | {0.00} | 0.24 | 4.11E+05 |
| *n*1807—18a | Zoned | 1891 | 7 | 1827 | 12 | 1771 | 20 | 0.1157 | 0.4 | 5.043 | 1.4 | 0.3161 | 1.3 | 0.96 | −4.2 | 336 | 143 | 132 | 0.31 | 0.39 | 6.05E+03 |
| *n*1807—19a | Zoned, pale outer domain | 1888 | 9 | 1846 | 12 | 1809 | 21 | 0.1155 | 0.5 | 5.159 | 1.4 | 0.3239 | 1.3 | 0.94 | −1.4 | 202 | 68 | 79 | 0.28 | 0.31 | 6.74E+03 |
| *n*1807—20a | Darker inner domain | 1903 | 12 | 1853 | 13 | 1809 | 21 | 0.1165 | 0.7 | 5.205 | 1.5 | 0.3240 | 1.3 | 0.89 | −1.6 | 146 | 41 | 57 | 0.89 | 0.26 | 2.10E+03 |
| *n*1807—21a | Zoned | 1892 | 10 | 1836 | 12 | 1786 | 21 | 0.1158 | 0.5 | 5.097 | 1.4 | 0.3193 | 1.3 | 0.92 | −2.9 | 346 | 116 | 134 | 0.34 | 0.32 | 5.46E+03 |
| *n*1807—22a | Zoned | 1882 | 7 | 1861 | 12 | 1841 | 21 | 0.1152 | 0.4 | 5.249 | 1.4 | 0.3306 | 1.3 | 0.96 | | 344 | 113 | 137 | 0.28 | 0.31 | 6.65E+03 |
| *n*1807—23a | Zoned | 1869 | 8 | 1871 | 12 | 1873 | 21 | 0.1143 | 0.5 | 5.316 | 1.4 | 0.3372 | 1.3 | 0.95 | | 409 | 180 | 171 | 0.14 | 0.43 | 1.38E+04 |
| *n*1807—24a | Zoned | 1877 | 9 | 1874 | 12 | 1872 | 21 | 0.1148 | 0.5 | 5.332 | 1.4 | 0.3369 | 1.3 | 0.94 | | 259 | 71 | 104 | 0.15 | 0.27 | 1.25E+04 |
| *n*1807—25a | Zoned | 1883 | 6 | 1887 | 12 | 1892 | 22 | 0.1152 | 0.3 | 5.417 | 1.4 | 0.3411 | 1.3 | 0.97 | | 367 | 107 | 150 | 0.05 | 0.29 | 3.52E+04 |

All errors are in 1 sigma level.

[a] Error correlation in conventional concordia space.

[b] Age discordance at closest approach of error ellipse to concordia (2σ level).

[c] Percentage of common $^{206}Pb$ in measured $^{206}Pb$, calculated from the $^{204}Pb$ signal assuming a present-day Stacey and Kramers (1975) model terrestrial Pb-isotope composition. Numbers in parentheses are given when no correction has been applied.

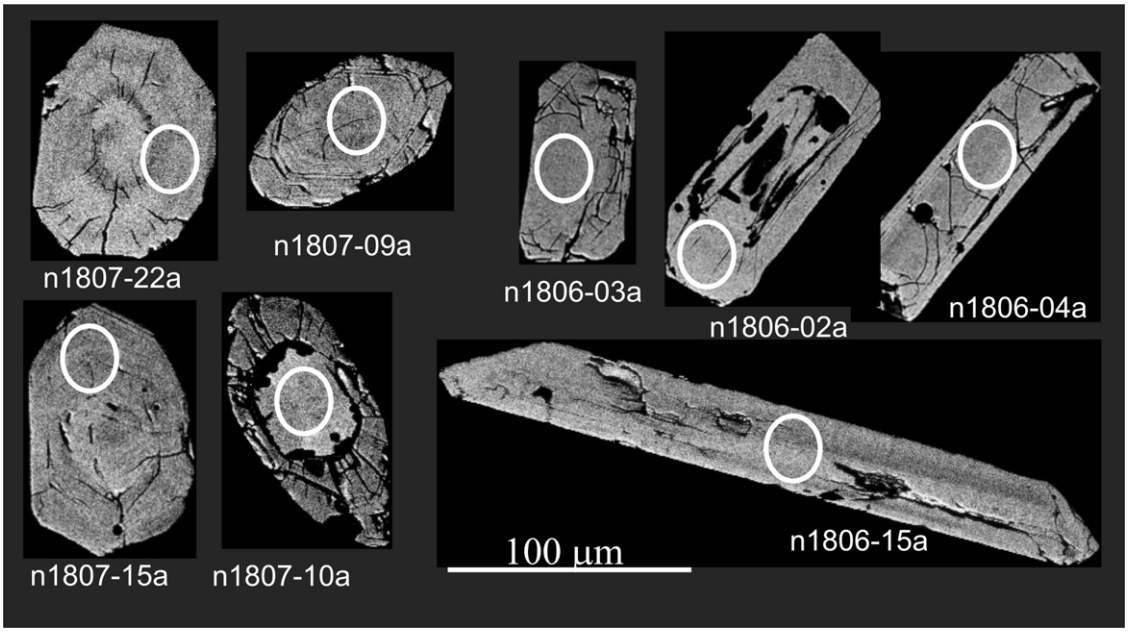


Fig. 8. Selected zircon BSE images. Dated zircon domains (ellipses) and corresponding analysis numbers are indicated (*n*1807: Fiskars intermediate dyke; *n*1806: Kuovila granodiorite).

zircons are generally very fractured and quite commonly have inclusions.

A total of 22 zircon domains were dated using ion microprobe (Table 1). Three analyses were rejected due to high common lead contents. The Th/U ratio varies only in small range; high U was measured from a structurally homogeneous rim and a homogeneous centre domain (Table 1, 9b and 16a). On a concordia diagram (Fig. 9), all the data irrespective of the analysed zircon type or domain plot in a cluster. A few analyses show minor discordance. The concordant analyses determine an age of 1877 ± 3 Ma ($n = 14/19$) for the Kuovila granodiorite and, therefore, give an age for the $D_2$ deformation in the Kuovila sub-area.

### 4.3. Fiskars intermediate dyke (n1807)

The Fiskars intermediate dyke sample yielded a very small amount of mostly stubby, pale brown, and transparent to translucent zircon. A few longer prismatic, paler, and more turbid crystals were found. In the BSE images (Fig. 8) the zircons principally show magmatic zoning. Two grains have structurally homogeneous cores (Fig. 8, 10a) with high U concentrations. However, the

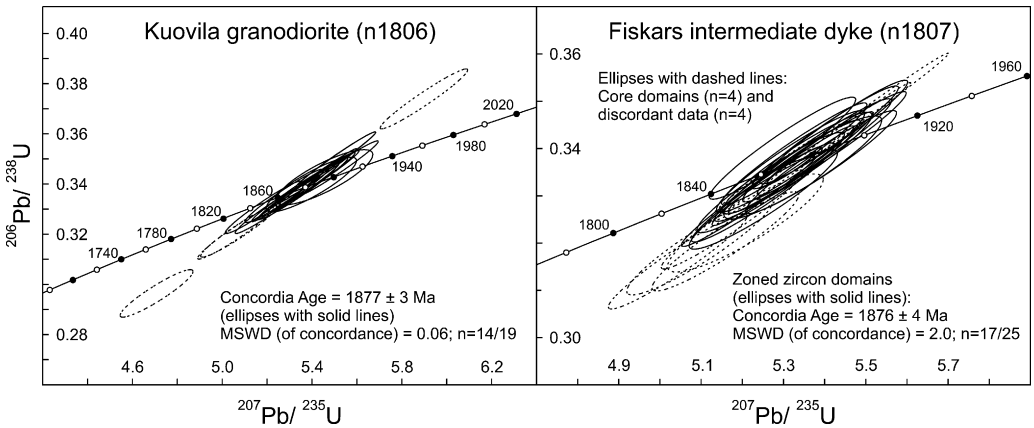


Fig. 9. Concordia diagrams showing zircon U–Pb isotopic data for the Kuovila granodiorite (*n*1806) and the Fiskars intermediate dyke (*n*1807).

rims around the cores were too thin or fractured for any decent U–Pb analysis (Fig. 8). Furthermore, one zircon (Table 1, 05a) with zoned core and structurally homogeneous, altered rim was found.

A total of 25 zircon domains from the sample were dated (Table 1). The data are mostly concordant and the range in Th/U is small when the two analyses from homogenised core domains are excluded. On a concordia diagram (Fig. 9), all the U–Pb isotopic data plot in a tight cluster. The concordant data from zoned zircon domains apparently determines an age of $1876 \pm 4$ Ma ($n = 17/25$) for the dyke. The data from core domains plot on that same cluster. In the Fiskars sub-area, the intermediate dyke determines an age of $1876 \pm 4$ Ma for the $D_2$ deformation.

## 5. Discussion

### 5.1. Deformation mechanisms

The observed strain patterns set constraints for the deformation mechanisms, which caused the preservation of the early structures. These constraints further provide information on the tectonic regime during the deformations. The lower cumulative strain in the Orijärvi sub-area relative to the intensely $D_2$- and $D_3$-folded area to the east, results from polyphase strain partitioning that initiated during $D_2$ and continued during $D_3$ and $D_4$. The $D_2$ structures were originally upright in the Orijärvi sub-area, which becomes evident as the metamorphic mineral growth during $D_2$ shows no variations across the Orijärvi synform–antiform structure (this study; Eskola, 1914). Pressures deviating from the estimated 3–5 kbar (Schreurs and Westra, 1986) across the fold structure with a wavelength of ~10 km would be expected if the $D_2$ synform–antiform pair originally was a recumbent fold, presently $D_3$-refolded into an upright position. In contrast to the upright $D_2$ in the Orijärvi sub-area, $D_2$ structures in the Iso-Kisko and Fiskars sub-areas were sub-horizontal as revealed by the sub-horizontal $S_2$ enveloping surface.

The upright $D_2$ structure in the Orijärvi sub-area therefore represents an anomalous orientation within the generally sub-horizontal early Svecofennian thrust tectonic regime within the Uusimaa belt (Van Staal and Williams, 1983; Ehlers et al., 1993). We think that this anomalous orientation resulted when $D_2$ strain was partitioned as a function of crustal depth; sub-horizontal high-

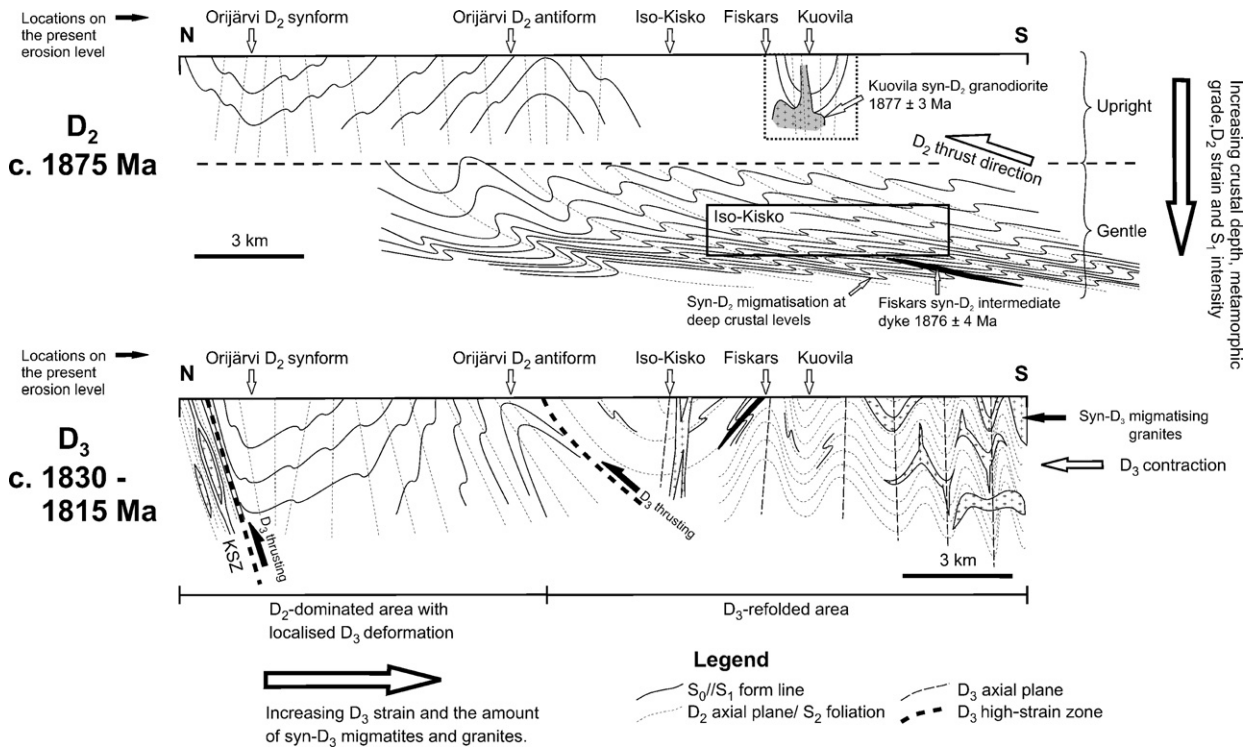


Fig. 10. Geometry of the deformation structures across the preserved domain after $D_2$ and $D_3$ deformations. The shown locations along the present erosion level illustrate how $D_3$ deformation displaced the $D_2$ structures into their present positions. Kuovila sub-area omitted for clarity in the lower part of the figure.

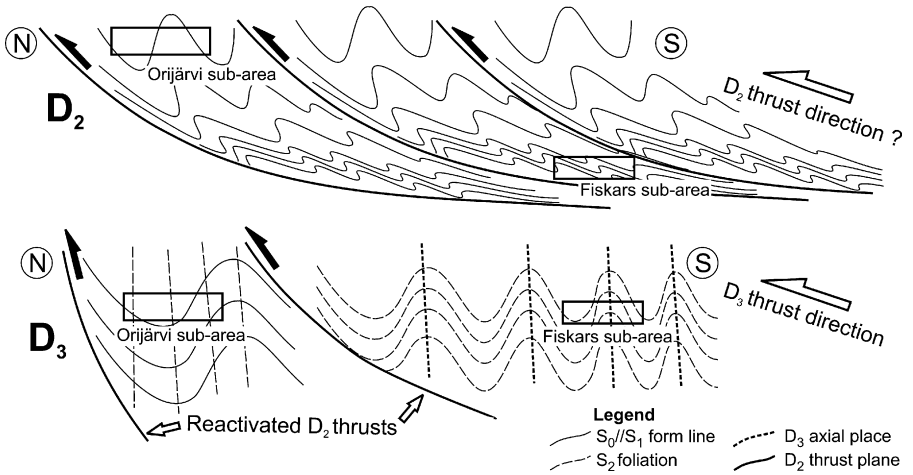


Fig. 11. Schematic model to explain the deformation mechanisms during $D_2$ and $D_3$ in the study area.

strain structures were formed at depth (the Fiskars and Iso-Kisko sub-areas) whereas upright low-strain structures were formed at higher crustal levels (the Orijärvi sub-area; Fig. 10). This may be explained by two mechanisms: (1) Continuous thrusting where continued contraction and detachment in the upper plate above the sheared base led to progressive steepening of the $F_2$ folds (Fig. 11). (2) Shearing along a sub-horizontal shear zone at deep crustal levels whilst the upper crust experienced contractional folding. The first alternative is supported by the observed $D_2$ thrust in the Kemiö area (Fig. 1; Van Staal and Williams, 1983) and the commonly observed progressive changes of the fold axial surface orientations in thrust tectonic environments (e.g. Ramsay and Huber, 1987, pp. 377–378). Therefore, the first mechanism is more likely considered responsible for the strain patterns during $D_2$.

Structures in the Kuovila sub-area are similar to the Orijärvi sub-area and these two sub-areas are therefore considered to represent similar crustal depths as also interpreted by Skyttä et al. (2005). The correlation of increasing $D_2$ strain, metamorphic grade during $D_2$, and the intensity of $S_1$ fabric with increasing crustal depth (Fig. 10) is similar to what was observed in the Tampere-Vammala area to the north of the present study area (Fig. 1; Kilpeläinen, 1998). The Fiskars sub-area apparently shows the deepest and the Orijärvi and Kuovila sub-areas the shallowest crustal depths in the area during $D_2$. Besides the crustal depth, the migmatisation during $D_2$ in the Fiskars area was possibly partly induced by a contact-metamorphic effect of the ~1875 Ma magmatism as presented in this paper.

Strain partitioning during $D_3$ was controlled by the geometry of the $D_2$ structures, therefore accounting for the low cumulative strain in the Orijärvi sub-area; the areas with gently dipping $D_2$ structures were refolded into upright $F_3$ folds, but the already upright Orijärvi sub-area acted as an almost rigid block resulting in strain partitioning into $D_3$ high-strain zones on the block margins. This is suggested to initiate the Kisko shear zone deformation and $D_3$ thrusting along the contact of the Iso-Kisko and Orijärvi sub-areas (Fig. 10). These both probably were $D_2$ thrust/detachment planes that were reactivated during $D_3$. Within the $D_3$-refolded areas, the $D_3$ strain intensity increases laterally to the south, as does the amount of syn-$D_3$ migmatites, granites and pegmatites. This is at least partly due to the block movements during $D_4$, which brought up the deeper crust in the south. The variation of $S_2$ dips in the western part of the Iso-Kisko sub-area indicates that doming, similar to that reported elsewhere in the Uusimaa belt (Härme, 1954; Bleeker and Westra, 1987), took place in the present study area during $D_3$.

Syn-$D_3$ migmatisation (Fig. 10) is widely present in the Fiskars sub-area rocks, whereas the Iso-Kisko sub-area only contains some axial-planar pegmatite dykes. The expression of metamorphism during $D_3$ in the Orijärvi sub-area is the growth of $And_2$ over the $S_2$ foliation, and possibly also the Sill, which replaces $And_2$ grains at the margins. The generally sluggish polymorphic transition of andalusite to sillimanite (e.g. Pattison, 1992; Cesare et al., 2002) was, therefore probably catalysed by strain during $D_3$. Partial melting conditions were not met in the Orijärvi sub-area. It is principally possible that the $And_2$ and sillimanite porphyroblasts grew during the late stages of $D_2$. This is, however, inconsistent with the $1798 \pm 3$ Ma titanite age from the Orijärvi synform (Väisänen and Mänttäri, 2002), which proba-

bly indicates prolonged cooling after the high heat flow at ~1840–1815 Ma. The peak-metamorphic monazite age from a non-migmatitic rock in the Kemiö area at 1824 ± 5 Ma (Levin et al., 2005) also supports strong late Svecofennian thermal overprint in the Orijärvi area. Therefore, the Orijärvi sub-area was largely preserved from the $D_3$ deformation but did, however, experience a new stage of metamorphic mineral growth during $D_3$.

$D_4$ deformation was predominantly retrograde and localised into distinct shear zones, which define separate crustal domains: the preserved domain between the Kisko and Jyly shear zones and the late Svecofennian migmatitic domain outside the shear zones. The close association of the pegmatite dykes with folding in the Jyly and Kisko shear zones is consistent with the at least some shear zone deformation during or soon after the late Svecofennian peak-metamorphic conditions, and progressive evolution during $D_4$, as also indicated by the previous studies (Ploegsma, 1989; Ploegsma and Westra, 1990). The regional structural evolution nevertheless implies that the shear zones likely initiated already during $D_2$ or $D_3$ as discussed above, but direct evidence for this is lacking. $D_4$ and the following brittle reactivation along the Kisko and Jyly shear zones juxtaposed the neighbouring crustal blocks into their present position.

### 5.2. Deformation kinematics

The $F_2$ folds most probably resulted from SSE–NNW oriented $D_2$ contraction, which is supported by the steeply NE- and SW-plunging $F_2$ fold axes in the Fiskars area, which therefore indicate $D_3$ refolding of subhorizontal, NE–ENE and SW–WSW striking $F_2$ fold axes. Similar $D_2/D_3$ interference is also evident in the Kemiö area: $F_2$ fold axes plunge moderately to steeply towards WSW on the southern limb of a large-scale east–west trending $F_3$ antiform (Verhoef and Dietvorst, 1980) and gently to moderately towards NE–ENE on the northern limb of the antiform (Levin et al., 2005). The regional pattern of the $D_2/D_3$ refolding would, therefore suggest that the NE–ENE trending $D_2$ structures in the Orijärvi $D_2$ synform would stand for the original orientation of the $F_2$ folding, and the E–W orientation elsewhere is a result of $D_3$ transposition. Ploegsma and Westra (1990) considered $D_2$ ($D_1$ in their study) to have an ESE to SSE vergence. However, the upright $D_2$ synform–antiform structure in the Orijärvi sub-area, which they did not recognize, is not consistent with such an interpretation. The present data does not allow us to make a reliable argument for the $D_2$ thrust direction, as the intensity of $D_3$ refolding in the southern part of the study area widely inhibits recognition of the location relative to the $F_3$ folds, i.e. on which limb the $D_2$ structure is located. However, the identified $D_2$ contraction direction is consistent with the observed $D_2$ vergences towards west and north in the Kemiö area (Ehlers et al., 1993). Therefore, we suggest that $D_2$ related to NNW-directed tectonic transport.

Recognition of the originally upright $D_2$ structures in the Orijärvi sub-area indicates that the constrictional strain is either related to layer-parallel slip during $D_2$ or to localised deformation during $D_1$; the latter was considered responsible for the constriction in the Kuovila area (Skyttä et al., 2005). A pre-$D_2$ origin for the constriction is also favoured by the suggested plutonic diapirism as a possible reason for the constriction (Stel et al., 1999), because plutonism in the Orijärvi area was synvolcanic (Väisänen et al., 2002) and the later, syn-$D_3$ doming, such as in the Mustio (Härme, 1954; Bleeker and Westra, 1987) and in the Iso-Kisko areas, did not affect the Orijärvi sub-area.

The upright $F_3$ folds within and outside the preserved domain indicate approximately north–south compression during $D_3$, which also probably involved thrusting towards north, suggested by: (1) overturning of the Orijärvi antiform, (2) deeper crustal section presently exposed in the south (Fig. 10), and (3) orientation of the high-strain zone and the related mineral lineations along the contact of the Iso-Kisko and Orijärvi sub-areas. This is consistent with the models of transpressive deformation both in the Svecofennian of southern Finland (Ehlers et al., 1993; Lindroos et al., 1996) and central Sweden (Högdahl and Sjöström, 2001).

East-side-up movements during $D_4$ explain the change in metamorphic grade across the Jyly shear zone. This faulting was ultimately responsible for the preservation of the $D_2$ structures, as it juxtaposed the strongly migmatitic deeper crust on the eastern side and the preserved domain on the western side of the shear zone. Approximately east–west contraction, probably west-vergent thrusting, is consistent with the reverse dip-slip movements along the main shear zones, the Kisko and Jyly shear zones, and with the localised west-vergent thrust-folds in the northernmost part of the Orijärvi sub-area (Fig. 5g). Strong curving of the $S_2$ planes in the northernmost part of the sub-area may be caused by subvertical corner flow in the vicinity of the intersecting shear zones (see Mandal et al., 2002).

In conclusion, the two contractional main folding events, $D_2$ and $D_3$, were separated by ~45 Ma, and probably were related to thrusting towards N–NW. Thrusting is supported by field evidence (Ehlers et al., 1993; Väisänen and Hölttä, 1999) and particularly by seismic profiles that display subhorizontal stacking structures

in southwestern Finland (Korja and Heikkinen, 2005). $D_2$ and $D_3$ represent different episodes of deformation as suggested by Lahtinen et al. (2005), rather than one semi-continuous orogenic event (Gorbatschev and Bogdanova, 1993). The presence of the sub-horizontally foliated granite, boudinage of the main foliation and the related vertical shortening recorded by the folded leucosome veins in the Fiskars sub-area may be the expression of the suggested extensional event intermediate between $D_2$ and $D_3$, i.e. at ~1.86–1.84 Ga (see Lahtinen et al., 2005; Bergman et al., 2006; Nironen and Lahtinen, 2006). Also the recent datings of granites at ~1.85 Ga (Kurhila et al., 2005) likely indicate that some granitic magmatism pre-dates the main stage of the contractional late Svecofennian $D_3$ deformation and may, therefore, be syntectonic with the extension. $D_4$ followed soon after $D_3$, but there was a shift in the regional stress field from north–south into more east–westerly direction at least within this part of the Uusimaa belt, as show by the predominant dip-slip nature of the Jyly shear zone. This is consistent with the dextral tranpressive models by Ehlers et al. (1993) and Cagnard et al. (2006). In their model based on analogue experiments, Cagnard et al. (2006) assumed the homogeneous crust more or less in the same high metamorphic condition, which leads to ductile sub-horizontal flow without thrusting. The crust in southwestern Finland, however, is highly heterogeneous including granulite facies migmatitic areas, non-migmatitic volcanic areas and areas with predominantly plutonic rocks. In addition, as pointed out by Korja and Heikkinen (2005), exotic microcontinents might have been involved in the accretionary process. All combined, great contrast differences allow thrusting to take place, as documented by Korja and Heikkinen (2005).

### *5.3. Comparison between the Orijärvi and the Tampere-Vammala areas*

Characteristic for the early evolution both in the Tampere-Vammala area (Nironen, 1989; Kilpeläinen, 1998) and the Orijärvi area is that the metamorphic grade is controlled by the crustal depth, and that the deeper parts have more intense early fabrics in comparison with the shallower parts. The deepest crustal depths were migmatised and sub-horizontally deformed either locally (Orijärvi) or in wider areas (Vammala). Both in the Orijärvi and Tampere-Vammala areas the competent volcanic formations only recorded upright folding with large wavelengths. Despite the similarities between the two areas, there is a major difference in that all the deformation in the Tampere-Vammala area was early Svecofennian while the Orijärvi area also experienced major late Svecofennian overprinting. In summary, preservation of the low-grade rocks both in the Orijärvi and Tampere areas can be explained by the upright geometry of structures, which caused subsequent strain localisation on the margins of the upright domains (Fig. 12 in Nironen (1989); this study).

## 6. Conclusions

1. The early Svecofennian $D_2$ deformation within the Uusimaa belt took place ~1875 Ma ago.
2. Preservation of the early Svecofennian structures in the Orijärvi area resulted from polyphase strain partitioning. $D_2$ strain was partitioned as a function of crustal depth; sub-horizontal high-strain domains were formed at deep crustal levels and upright low-strain domains were formed at higher crustal levels. Also the metamorphic grade during $D_2$ correlated with crustal depth; local migmatisation took place at the deepest crustal levels. The orientation of $D_2$ structures controlled the further strain partitioning during $D_3$; the areas with gentle $D_2$ structures were refolded into upright $F_3$ folds, whereas the areas with upright $D_2$ structures were acting as almost rigid blocks causing strain partitioning into high-strain zones along the block margins. This explains the preservation of the early Svecofennian structures in the Orijärvi area. $D_4$ deformation was localised into dip-slip shear zones causing crustal block movements, which juxtaposed the migmatitic and the preserved domains.
3. The similarities in the structural evolution in the Orijärvi and Tampere-Vammala areas indicate that the upright early Svecofennian structures in southern Finland caused pronounced strain partitioning during subsequent deformations.

## Acknowledgements

We wish to express our gratitude to Rod Holcombe and Mikko Nironen for instructive comments on the manuscript. The comments by two anonymous reviewers greatly helped to improve the manuscript. Martin Whitehouse, Lev Ilyinsky and Bodil Kajrup from the Nordsim laboratory are thanked for all the help with the Nordsim dating. The Nordsim facility is financed and operated under an agreement between the research councils of Denmark, Norway and Sweden, the Geological Survey of Finland and the Swedish Museum of Natural History. This is Nordsim publication #158. The Finnish Graduate School in Geology and GTK funded this work.

## References


Allen, R.L., Lundström, I., Ripa, M., Simeonov, A., Christofferson, H., 1996. Facies analysis of a 1.9 Ga, continental margin, back-arc, felsic caldera province with diverse Zn–Pb–Ag–(Cu–Au) sulfide and Fe oxide deposits, Bergslagen Region, Sweden. Econ. Geol. 91, 979–1008.

Bergman, S., Högdahl, K., Nironen, M., Lundqvist, L., Sjöström, H., Ogenhall, E., Lahtinen, R., 2006. Detrital zircons in late Svecofennian metasandstones in central Sweden and southern Finland. Bull. Geol. Soc. Finland, Special Issue 1, 16.

Bleeker, W., Westra, L., 1987. The evolution of the Mustio gneiss dome, Svecofennides of SW Finland. Precambrian Res. 36, 227–240.

Cagnard, F., Durrieu, N., Gapais, D., Brun, J.-P., Ehlers, C., 2006. Crustal thickening and lateral flow during compression of hot lithospheres, with particular reference to Precambrian times. Terra Nova 18, 72–78.

Carreras, J., Druguet, E., Griera, A., 2005. Shear zone-related folds. J. Struct. Geol. 27, 1229–1251.

Cesare, B., Gómez-Pugnaire, M.T., Sánchez-Navas, A., Grobety, B., 2002. Andalusite–sillimanite replacement (Mazarrón, SE Spain): a microstructural and TEM study. Am. Miner. 87, 433–444.

Colley, H., Westra, L., 1987. The volcano-tectonic setting and mineralization of the early Proterozoic Kemiö-Orijärvi-Lohja belt, SW Finland. In: Pharaoh, T.C., Beckinsale, R.D., Rickard, D. (Eds.), Geochemistry and Mineralizations of Proterozoic Volcanic Suites. Geological Society Special Publications 33, pp. 95–107.

Ehlers, C., Lindroos, A., Selonen, O., 1993. The late Svecofennian granite–migmatite zone of southern Finland—a belt of transpressive deformation and granite emplacement. Precambrian Res. 64, 295–309.

Ehlers, C., Skiöld, T., Vaasjoki, M., 2004. Timing of Svecofennian crustal growth and collisional tectonics in Åland, SW Finland. Bull. Geol. Soc. Finland 76, 63–91.

Eskola, P., 1914. On the petrology of the Orijärvi region in southwestern Finland. Bulletin de la Commission Géologique de Finlande 40, 277 pp.

Eskola, P., 1915. Om sambandet mellan kemisk och mineralogisk sammansättning hos Orijärvi traktens metamorfa bergarter. English summary: On the relations between the chemical and mineralogical composition in the metamorphic rocks of the Orijärvi region. Bulletin de la Commission Géologique de Finlande 44, 145 pp.

Gaál, G., 1990. Tectonic styles of early Proterozoic ore deposition in the Fennoscandian Shield. Precambrian Res. 46, 83–114.

Gorbatschev, R., Bogdanova, S., 1993. Frontiers in the Baltic Shield. Precambrian Res. 64, 3–21.

Härme, M., 1954. Structure and stratigraphy of the Mustio area, southern Finland. Bulletin de la Commission Géologique de Finlande 166, 29–48.

Hietanen, A., 1975. Generation of potassium-poor magmas in the northern Sierra Nevada and Svecofennian of Finland. Geol. Soc. Am. Bull. 58, 1019–1085.

Högdahl, K., Sjöström, H., 2001. Evidence for 1.82 Ga transpressive shearing in a 1.85 Ga granitoid in central Sweden: implications for the regional evolution. Precambrian Res. 105, 37–56.

Hopgood, A.M., Bowes, D.R., Kouvo, O., Halliday, A.N., 1983. U–Pb and Rb–Sr isotopic study of polyphase deformed migmatites in the Svecokarelides, southern Finland. In: Atherton, M.P., Gribble, C.D. (Eds.), Migmatites, Melting and Metamorphism. Shiva, Cheshire, pp. 80–92.

Huhma, H., 1986. Sm–Nd, U–Pb and Pb–Pb isotopic evidence for the origin of the Early Proterozoic Svecokarelian crust in Finland. Geol. Survey Finland Bull. 337, 48 pp.

Jurvanen, T., Eklund, O., Väisänen, M., 2005. Generation of A-type granitic melts during the late Svecofennian metamorphism in southern Finland. GFF 127, 139–147.

Kilpeläinen, T., 1998. Evolution and 3D modelling of structural and metamorphic patterns of the Palaeoproterozoic crust in the Tampere-Vammala area, southern Finland. Geol. Survey Finland Bull. 397, 124 pp.

Korja, A., Heikkinen, P., 2005. The accretionary Svecofennian orogen—insight from the BABEL profiles. Precambrian Res. 136, 241–268.

Korsman, K., Koistinen, T., Kohonen, J., Wennerström, M., Ekdahl, E., Honkamo, M., Idman, H., Pekkala, Y. (Eds.), 1997. Bedrock Map of Finland 1:1 000 000. Geological Survey of Finland, Espoo.

Korsman, K., Korja, T., Pajunen, M., Virransalo, P., GGT/SVEKA Working Group, 1999. The GGT/SVEKA Transect: structure and evolution of the continental crust in the Paleoproterozoic Svecofennian Orogen in Finland. Int. Geol. Rev. 41, 287–333.

Kurhila, M., Vaasjoki, M., Mänttäri, I., Rämö, T., Nironen, M., 2005. U–Pb ages and Nd isotope characteristics of the lateorogenic, migmatizing microcline granites in southwestern Finland. Bull. Geol. Soc. Finland 77, 105–128.

Lahtinen, R., 1996. Geochemistry of Palaeoproterozoic supracrustal and plutonic rocks in the Tampere-Hämeenlinna area, southern Finland. Geol. Survey Finland Bull. 389, 113 pp.

Lahtinen, R., Korja, A., Nironen, M., 2005. Paleoproterozoic tectonic evolution. In: Lehtinen, M., Nurmi, P.A., Rämö, O.T. (Eds.), Precambrian Geology of Finland—Key to the Evolution of the Fennoscandian Shield. Elsevier Science B.V., Amsterdam, pp. 481–532.

Latvalahti, U., 1979. Cu–Zn–Pb ores in the Aijala-Orijärvi area, Southwest Finland. Econ. Geol. 79, 1035–1059.

Levin, T., Engström, J., Lindroos, A., Baltybaev, S., Levchenkov, O., 2005. Late-Svecofennian transpressive deformation in SW Finland—evidence from late-stage D3 structures. GFF 127, 129–137.

Lindroos, A., Ehlers, C., 1994. Emplacement, deformation and geochemistry of bimodal volcanics in Vestlax, SW Finland. Geol. Survey Finland, Special Paper 19, 173–184.

Lindroos, A., Romer, R.L., Ehlers, C., Alviola, R., 1996. Late-orogenic Svecofennian deformation in SW Finland constrained by pegmatite emplacement ages. Terra Nova 8, 567–574.

Ludwig, K.R., 2003. Isoplot/Ex 3. A Geochronological Toolkit for Microsoft Excel. Special Publication No. 4. Berkeley Geochronology Center.

Mandal, N., Samanta, S.K., Chakraborty, C., 2002. Flow and strain patterns at the terminations of tapered shear zones. J. Struct. Geol. 24, 297–309.

Mouri, H., Väisänen, M., Huhma, H., Korsman, K., 2005. Sm–Nd garnet and U–Pb monazite dating of high-grade metamorphism and crustal melting in the West Uusimaa area, southern Finland. GFF 127, 123–128.

Nironen, M., 1989. The Tampere Schist Belt: structural style within an early Proterozoic volcanic arc system in southern Finland. Precambrian Res. 43, 23–40.

Nironen, M., 1997. The Svecofennian Orogen: a tectonic model. Precambrian Res. 86, 21–44.

Nironen, M., 1999. Structural and magmatic evolution in the Loimaa area, southwestern Finland. Bull. Geol. Soc. Finland 71, 57–71.

Nironen, M., Lahtinen, R., 2006. Late Svecofennian sedimentary-volcanic association at Pyhäntaka, southern Finland. Bull. Geol. Soc. Finland, Special Issue 1, 109.

Passchier, C.W., Trouw, R.A.J., 1996. Microtectonics. Springer Verlag, Berlin, 289 pp.

Patchett, P.J., Kouvo, O., 1986. Origin of continental crust of 1.9–1.7 Ga age; Nd isotopes and U–Pb zircon ages in the Svecokarelian terrain of South Finland. Contrib. Miner. Petrol. 92, 1–12.

Pattison, D.R.M., 1992. Stability of andalusite and sillimanite and the $Al_2SiO_5$ triple point: constraints from the Ballachulish aureole, Scotland. J. Geol. 100, 423–446.

Ploegsma, M., 1989. Shear zones in the West Uusimaa area, SW Finland. PhD Thesis. Vrije Universiteit te Amsterdam, 134 pp.

Ploegsma, M., Westra, L., 1990. The Early Proterozoic Orijärvi triangle (southwest Finland): a key area on the tectonic evolution of the Svecofennides. Precambrian Res. 47, 51–69.

Ramsay, J.G., Huber, M.I., 1987. The Techniques of Modern Structural Geology, vol.2: Folds and Fractures. Academic Press, London, pp. 309–700.

Reinikainen, J., 2001. Petrogenesis of Paleoproterozoic marbles in the Svecofennian Domain, Finland. Geological Survey of Finland, Report of Investigations 154, 84 pp.

Schneiderman, J.S., Tracy, R.T., 1991. Petrology of ortoamphibolite-cordierite gneisses from the Orijärvi area, southwest Finland. Am. Miner. 76, 942–955.

Schreurs, J., Westra, L., 1986. The thermotectonic evolution of a Proterozoic, low pressure, granulite dome, West Uusimaa, SW Finland. Contrib. Miner. Petrol. 93, 236–250.

Schumacher, J.C., Czank, M., 1987. Mineralogy of triple- and double-chain pyriboles from Orijärvi, southwest Finland. Am. Miner. 72, 345–352.

Skyttä, P., Käpyaho, A., Mänttäri, I., 2005. Supracrustal rocks in the Kuovila area, Southern Finland: structural evolution, geochemical characteristics and the age of volcanism. Bull. Geol. Soc. Finland 77, 129–150.

Suominen, V., 1991. The chronostratigraphy of southwestern Finland with special reference to Postjotnian and Subjotnian diabases. Geol. Survey Finland Bull. 356, 100 pp.

Stacey, J.S., Kramers, J.D., 1975. Approximation of terrestrial lead isotope evolution by a two-stage model. Earth Planet. Sci. Lett. 26, 207–221.

Stel, H., Van Rees, D., Schenke, B., 1999. Strain analysis in the Orijärvi triangle, southwestern Finland; in perspective of tectonic models. Bull. Geol. Soc. Finland 71, 329–337.

Torvela, T., Annersten, H., 2005. PT-conditions of deformation within the Palaeoproterozoic South Finland shear zone: some geothermobarometric results. Bull. Geol. Soc. Finland 77, 151–164.

Vaasjoki, M., 1994. Valijärven hapan vulkaniitti: minimi Hämeen liuskejakson iäksi. English summary: radiometric age of a meta-andesite at Valijärvi, Häme schist zone, southern Finland. Geologi 46, 91–92.

Väisänen, M., Hölttä, P., 1999. Structural and metamorphic evolution of the Turku migmatite complex, southwestern Finland. Bull. Geol. Soc. Finland 71, 177–218.

Väisänen, M., Mänttäri, I., 2002. 1.90–1.88 Ga arc and back-arc basin in the Orijärvi area, SW Finland. Bull. Geol. Soc. Finland 74, 185–214.

Väisänen, M., Mänttäri, I., Hölttä, P., 2002. Svecofennian magmatic and metamorphic evolution in southwestern Finland as revealed by U–Pb zircon SIMS geochronology. Precambrian Res. 116, 111–127.

Väisänen, M., Mänttäri, I., Kriegsman, L.M., Hölttä, P., 2000. Tectonic setting of post-collisional magmatism in the Palaeoproterozoic Svecofennian Orogen, SW Finland. Lithos 54, 63–81.

Van Staal, C.R., Williams, P.F., 1983. Evolution of a Svecofennian-mantled gneiss dome in SW Finland, with evidence for thrusting. Precambrian Res. 21, 101–128.

Verhoef, P.N.W., Dietvorst, E.J.L., 1980. Structural analysis of differentiated schists and gneisses in the Taalintehdas area, Kemiö Island, southwest Finland. Bull. Geol. Soc. Finland 52, 147–164.

Weihed, P., Arndt, N., Billström, K., Duchesne, J.-C., Eilu, P., Martinsson, O., Papunen, H., Lahtinen, R., 2005. 8: Precambrian geodynamics and ore formation: the Fennoscandian Shield. Ore Geol. Rev. 27, 273–322.

Whitehouse, M.J., Claesson, S., Sunde, T., Vestin, J., 1997. Ion microprobe U–Pb zircon geochronology and correlation of Archaean gneisses from the Lewisian complex of Gruinard Bay, northwestern Scotland. Geochim. Cosmochim. Acta 61, 4429–4438.

Whitehouse, M.J., Kamber, B., Moorbath, S., 1999. Age significance of U–Th–Pb zircon data from early Archaean rocks of west Greenland—a reassessment based on combined ion-microprobe and imaging studies. Chem. Geol. 160, 201–224.

Wiedenbeck, M., Allé, P., Corfu, F., Griffin, W.L., Meier, M., Oberli, F., von Quadt, A., Roddick, J.C., Spiegeln, W., 1995. Three natural zircon standards for U–Th–Pb, Lu–Hf, trace element and REE analysis. Geostandards Newsletter 19, 1–23.